

69-7760

MARINO, Andrew Anthony, 1941-  
DIELECTRIC AND PARAMAGNETIC RESONANCE  
PROPERTIES OF BONE.

Syracuse University, Ph.D., 1968  
Physics, solid state

University Microfilms, Inc., Ann Arbor, Michigan

DIELECTRIC AND PARAMAGNETIC RESONANCE PROPERTIES OF BONE

by

Andrew Anthony Marino

DISSERTATION

Submitted in partial fulfillment of the requirements for  
the degree of Doctor of Philosophy in Physics in the  
Graduate School of Syracuse University, June, 1968.

Approved CH Bachman

Date Feb 9 1968

## TABLE OF CONTENTS

I.	BONE AND ITS MAJOR COMPONENTS	
A.	Introduction .....	1
B.	Anatomical Structure of Bone .....	2
C.	Collagen .....	5
D.	Apatite .....	9
II.	DIELECTRIC CONSTANT AND BOUND WATER OF BONE	
A.	Introduction .....	16
B.	Experimental .....	21
1.	Sample preparation .....	21
2.	Apparatus .....	22
3.	Procedure .....	23
C.	Results .....	26
D.	Discussion .....	28
	Appendix A - Equations Used to Determine Dielectric Constant and Dielectric Loss .....	35
	Appendix B - Results of an Experiment on Patholog- ical Bone .....	37
	Appendix C - Method of Drying Employed .....	40
III.	ELECTRON PARAMAGNETIC RESONANCE STUDY OF BONE AND ITS MAJOR COMPONENTS	
A.	Introduction .....	42
B.	Preparation .....	43
C.	Results and Discussion	
1.	Bone .....	46

---

2. Collagen ..... 50

3. Apatite ..... 61

D. Conclusions ..... 69

Appendix A - Spectrographic Procedure ..... 79

Bibliography ..... 80

Acknowledgements ..... 85

Vita ..... 86

Table of Illustrations ..... 87

Illustrations

## I. BONE AND ITS MAJOR COMPONENTS

### Introduction

Bone is a highly specialized form of connective tissue that furnishes the skeletal support in most vertebrates. Considered as a material, and apart from its function in the body, bone is a solid, mechanically rigid substance having great stability. It is not a living tissue but rather is a product of a specialized cell termed an osteoblast. The actual cellular content of bone is quite small and represents no more than a perturbation to its chemical content and physical properties. A basic dissimilarity between bone and inorganic solids is that bone is not a unique material, but rather, for reasons that will soon be evident, a "class" of materials.

The most significant aspect of bone is precisely that it is a product, in part, of cell metabolism. One would like to understand the mechanisms by which bone production takes place. The clinical benefits that would derive from such knowledge are considerable. The work described herein is part of a broad program whose ultimate goal is the elucidation of the mechanisms involved in bone growth. The experiments are described after a brief introduction to the structure and organization of bone and its major components.

### Anatomical Structure of Bone

The following description of the anatomical structure of bone will be limited to the central region of the long bones (e.g. tibia, femur) and will not include the specialized apparatus found at the ends of these bones. Much of the following is however valid for bone in general. For a more complete description, the interested reader is referred to the text by Bloom and Fawcett (1).

Macroscopically, bone is found to be either cancellous or compact (cortical). (See Fig. 1). The latter is a hard continuous mass which gives the shaft (diaphysis) of the long bone its shape and mechanical rigidity, while the former is bone in the form of narrow rods of the order of a millimeter in thickness which interlace the marrow canal (medullary cavity). Cancellous bone emanates from and is contiguous with compact bone, and in the medullary cavity forms a sponge-like matrix whose interstices are filled with a layer of connective tissue (endosteum) and with bone marrow. In most instances, cancellous bone forms along the direction of maximum stress (2), and thus increases the strength to weight ratio of bone. The outer surface of the shaft is covered with a specialized connective tissue called the periosteum which is composed primarily of the fibrous protein collagen. The periosteum is attached to the shaft by collagen fibers which pass into the surface of the bone and appear to incorporate into the bone matrix. Also constituting part of the periosteum are the

(1) Bloom, W. and Fawcett, D.: Histology, Saunders Co., 1964.

(2) Glimcher, M.: Rev. Mod. Phy., 31, 361, (1959).

specialized bone cells known as osteoblasts and osteoclasts. The former are associated with the deposition of new bone such as in internal remodelling or fracture healing. The latter perform the function of resorption of bone. In addition, there is a third type of bone cell termed the osteocyte. Osteocytes are found in the interior of the compact shaft in small cavities called lacunae. They communicate with one another by means of narrow passages (canalicules) and with the outer surface of the shaft by means of the canals of Volkmann. The osteocytes are believed to be osteoblasts which have become sequestered in the interior and their exact role is not clearly understood. In the body, bone acts as a storehouse for inorganic ions, either adding or removing them from the vascular system in order to provide the required concentrations. One role of the osteocyte may be the regulation of this blood-bone exchange. Unlike the situation in most other tissue, the cells of bone form a negligibly small portion of the mass of bone. It has been estimated that there are approximately 20,000 osteocytes per cubic millimeter of compact bone (3).

Chemically, bone is composed of collagen, a fibrous protein, and apatite, an inorganic calcium phosphate salt. The nature of the chemical bond between the two, if any, is not understood. In addition to collagen and apatite, water is present in an amount inversely proportional to age and is about 3% of the weight

---

(3) Frost, H.: Bone Remodelling Dynamics, Thomas Co., 1963.

of mature cortical bone (3). The other components of bone, collectively called the "ground substance", include some ill-defined proteins and a number of carbohydrates known as the acid mucopolysacchrides. The ground substance of bone is on the whole very poorly characterized, particularly with regard to its function. The structure and relevant properties of both apatite and collagen will be discussed subsequently. For the present it suffices to point out that in terms of dry weight bone is approximately 65% apatite and 34% collagen, and thus the cellular content and ground substance taken together constitute less than 1% of the weight of bone, the majority of the 1% being the ground substance.

The basic structural unit of cortical bone is the osteon, which is an irregular cylinder whose axis is along the long axis of the bone. The osteon is composed of a central canal which contains a blood vessel (capillary) and successive layers (lamellae) which are roughly concentric with the central canal. Figure 2 illustrates the location of the osteons in cortical bone. Typically, the central canal might be 50 microns in diameter and surrounded by 15 lamellae of bone, each 5 microns in thickness. The collagen fibrils in an individual lamella spiral around the central canal with a pitch of about  $45^\circ$ . In the adjacent lamella the spiral is made in the opposite sense. The lacunae containing the osteocytes are distributed uniformly through the various lamellae. Cortical bone is essentially composed of an assembly

of osteons, with the irregular space between the osteons being occupied by incomplete or partially constructed osteons.

On the level of the electron microscope the apatite crystals of bone are seen to hexagonal rod shaped crystals of extremely small size. They are arranged in such a way that the crystallographic c-axis is approximately parallel to the fibril direction. Moreover, the crystals of the initial calcification phase appear to be spaced at regular intervals along the collagen fibers (4).

### Collagen

In addition to its presence in bone, collagen is found in living systems on practically all biological levels. It is the major fibrous constituent of skin, bone, tendon, fascia and other types of loose and dense connective tissue and is the most abundant protein in the human body. A great deal of research has been and continues to be done in an attempt to elucidate the structure and properties of collagen\*. Historically, interest in collagen was chiefly commercial, since being the chief constituent of animal skins, knowledge of its chemical properties was important in the tanning of leather. In addition, two of its degradation products, glue and gelatin, had found important commercial and industrial applications. In recent years however, research has indicated that collagen may be intimately involved in the aging process by undergoing a series of structural changes, hence, medical interest has been greatly stimulated. Also, a general class of

---

\* The last comprehensive review of the literature on collagen (Boransky, R., (1950) Guide to the Literature on Collagen, Bureau of Agricultural and Industrial Chem., Agricultural Research Administration, U.S.D.A., Eastern Regional Research Lab., Philadelphia) had over a thousand references. Since that time, the volume has increased enormously.

systematic disorders "the collagen diseases" has been found, comprising, in part, the rheumatic diseases and many disorders of joint and connective tissue.

Collagen, far from being a unique material, is actually a class of fibrous proteins consisting of (a) the cross-striated collagens (as seen in stained preparations in the electron microscope and in low angle X-ray diffraction) derived from the vertebrates, particularly the mammals, (b) the non-striated collagens derived from the invertebrates. All members of the class show the same wide angle X-ray diffraction pattern, and this is the chief basis for delineation of the class. Collagen from different sources does show variations in the low angle X-ray diffraction pattern but systematic coverage has not as yet been forthcoming. Furthermore, the X-ray diffraction pattern of collagen, both low and wide angle, has a marked dependence on degree of hydration of the fiber resulting in diffuse diffraction patterns, and tending to obscure the small differences that are seen.

Figure 3 illustrates the structural organization found in typical mammalian collagen. The complexity of the structure is immediately evident. The collagen fiber is seen to be composed of thinner parallel units called fibrils. Upon staining the fibrils exhibit the characteristic (of collagen) 640 A banding illustrated in Figure 3c. The fibril, in turn, is composed of still thinner units called protofibrils, which are columnar arrays

---

(4) Robinson, R.: J. Bone & Joint Surg., 34-A, 389, (1952).

of collagen molecules (tropocollagen) having an average diameter of from 10 A to about 16 A depending on the degree of hydration of the fiber (5).

In 1952, when the X-ray diffraction intensity distribution of a helical structure was determined theoretically (6), it became apparent that collagen possesses a helical structure. The number of individual polypeptide chains in the structure cannot be determined by X-ray diffraction alone, but Rich and Crick (7) feel that since it is not possible to stretch collagen more than 10% of its length, a single chain model is unlikely. Accordingly, and in consideration of a variety of experimental evidence, they proposed two closely related models for the structure of the tropocollagen macromolecule, designated Collagen I and Collagen II, each containing three polypeptide chains. The models were independently arrived at by Bear (8) and Ramachandran and Kartha (9), thus, there is general agreement by workers in the field that one of the two structures, probably Collagen II, is correct.

The models may be visualized by starting with the structures illustrated in Figure 4a which are projections perpendicular to the long axis of two polypeptide chains. Only the  $C_{\alpha}$  atoms are shown. Each of the chains has a left hand three-fold screw axis. The distance between adjacent residues (i.e. individual amino acids) in a single strand in the direction of the long axis is 3.1 A. Figure 4b and 4c illustrate the two different ways that

- 
- (5) Ramachandran, G.: International Review of Connective Tissue Research. Vol. I, Hall, D. (ed.), Academic Press, 1963, pg. 138.  
(6) Cochran, W., Crick, R., and Vand, V.: Acta Cryst., 5, 581, (1952).  
(7) Rich, A. and Crick, F.: J. Mol. Biol., 3, 483, (1961).  
(8) Bear, J.: Biophys. Biochem. Cytol., 2, 363, (1956).

three chains can be selected. Imagine that the group of three chains chosen is that shown in Figure 4b. The three chains are then deformed so that they slowly twist around a common axis in a gradual right hand helix. This gives the basic structure for Collagen I. If the group illustrated in Figure 4c had been chosen, then the Collagen II structure would have been arrived at. Figure 4d illustrates both the common axis and the axis of each polypeptide chain. The effect of giving the set of three chains a right hand twist is to alter the screw to  $108^\circ$  (from  $120^\circ$ ) and the translation to 2.86 A. The two coiled-coil structures differ chiefly in the direction and distribution of the hydrogen bonds which hold the three chains together. Rich has suggested that the two forms may be interconvertible by the application of stress.

Both Collagen I and Collagen II are theoretically able to accommodate any of a number of different amino acids without the basic structure being altered. Thus, the chemical variation of collagen from different sources can be explained on the basis of these models. In mammalian collagen, approximately one-third of the amino acid residues are glycine. Proline and hydroxyproline together make up about another one-third with the remaining third being the other amino acids (10). In the Rich-Crick models, every third residue is glycine, and the other lattice positions can accommodate a variety of amino acids corresponding to the variation in chemical composition of the different collagens.

---

(9) Ramachandran, G. and Kartha, G.: *Nature*, 176, 593, (1955).

(10) Gustavson, K.: The Chemistry and Reactivity of Collagen. Academic Press, 1956.

The models just described may correspond to only parts of the length of a protofibril, the other sections being regions of crystalline disorder, and thus they cannot be considered to be a final solution to the problem of the structure of collagen. Moreover, the models shed no light on the very interesting question of why some collagens calcify and turn to bone while others, tendon for example, do not calcify except in pathological situations.

#### Apatite

Bone mineral is a calcium phosphate salt containing in addition to  $\text{Ca}^{++}$  and  $\text{PO}_4^{=}$ ,  $\text{OH}^-$ , citrate, carbonate, water,  $\text{Na}^+$ ,  $\text{Mg}^+$ ,  $\text{K}^+$ ,  $\text{Cl}^-$ ,  $\text{F}^-$  (11), and other elements in trace amounts (12). Its crystalline nature was demonstrated by X-ray diffraction (XRD) in 1926 (13). In 1930 the structure of fluorapatite\*,  $\text{Ca}_{10}(\text{PO}_4)_6\text{F}_2$  (14), was determined by single crystal XRD. It became apparent that bone mineral has a crystal structure similar to that of the apatite class. Since the  $\text{OH}^-$  content of bone mineral is much greater than the  $\text{F}^-$  content and since the ionic radii of  $\text{OH}^-$  and  $\text{F}^-$  are about the same, it was generally assumed that bone mineral was similar to hydroxyapatite (HA),  $\text{Ca}_{10}(\text{PO}_4)_6(\text{OH})_2$ . The crystal structure of HA is illustrated in Figure 5.

The size of bone mineral crystals has been studied by XRD and electron microscopy and in all cases they are found to be exceedingly small. Carlstrom (15) finds by X-ray line broadening that the average dimension of bone mineral crystals along the

\* The only geological apatite found as a macrocrystal.

- (11) Posner, A.: Clin. Orthoped., 9, 5, (1957).
- (12) Ellis, E.: Ph.D. Dissertation, Syracuse University, (1964).
- (13) DeJong, W.: Rec. Trav. Chem., 45, 445, (1926).
- (14) Naray-Szabo, St.: Ztschr. Krist., 75, 387, (1930).

c-axis is about 230 A. The determination was made on powdered human cortical femur. Studies using an independent X-ray technique based on interpretation of diffuse low angle scatter showed that the crystals in intact bone were relatively uniform in size and rod shaped with average dimensions 210 x 75 A elongated in the c-axis direction (16, 17). Using electron microscopy, Robinson (4) measured 1,000 crystals of human bone mineral and gave as the average dimensions 500 x 200 x 100 A with the long dimension parallel to the c-axis. However, Carlstrom (15) has pointed out that the conditions normally employed in preparing a sample for study in the electron microscope, autoclaving and subsequent blending, may alter the crystal size. Later viewing intact bone, Robinson described bone crystals as tablets 200 x 200 x 20-50 A (18). Posner (11) reports that 25% of bone mineral crystals have dimensions larger than the average. In a review of all the evidence, Neuman and Neuman give the crystal size as 200 x 100 x 30-70 A (19). Thus, there is substantial agreement that the crystals of bone mineral are quite small, the largest average dimension reported being about 500 A. The question of the variation of crystal size with age, species, and location remains largely unexplored.

The atomic ratio of calcium to phosphorus\* (Ca/P) is theoretically 1.67 (10:6) for all apatites and there is no evidence from XRD to indicate the presence of water of crystallization. However,

---

\* Ratio of the number of atoms of calcium to phosphorus in a unit cell.

(15) Carlstrom, D.: Acta Radiol., Supp. 121, (1955).

(16) Engstrom, A. and Finean, J.: Nature, 171, 564, (1953).

(17) Finean, J. and Engstrom, A.: Biochim. Biophys. Acta, 11, 128, (1953).

the Ca/P of bone mineral is about 1.5 (19) and it loses a considerable amount of water when heated (2). These two facts have led to diverse names and various proposed structures for bone mineral and as a result the exact nature of bone mineral is still being debated. Neuman and Neuman (19) hold that bone mineral is HA and account for the aberrant stoichiometry by a combination of the following mechanisms: (a) substitution of one ion for another within the lattice, (b) presence of unsubstituted defects within the lattice, (c) surface substitution and absorption. In particular, they believe that an important process is the substitution of  $2\text{H}_3\text{O}^+$  for  $\text{Ca}^{++}$  up to a maximum of 4 hydroniums per unit cell. Starting with a  $\text{Ca-PO}_4\text{-H}_2\text{O}$  system, and depending on experimental conditions, such as pH and temperature, it is possible to produce synthetic HA with a Ca/P varying from 1.3 to more than 2.0, all of which possess an apatite XRD pattern and lose considerable amounts of water when heated. The weight loss experienced by these preparations when they are heated decreases linearly with increasing Ca/P from 1.3 to 1.67 and by just the amount one would expect under the assumption of a  $2\text{H}_3\text{O}^+$  substitution for  $\text{Ca}^{++}$ . Neuman and Neuman suggest that such a substitution occurs in bone mineral accounting, in part at least, for the low Ca/P and high water content. In their view, most of the "excess" water associated with bone mineral and synthetic preparations of HA is contained on the surface of these materials forming what they term the hydration shell, and is held by

---

(18) Robinson, R. and Watson, M.: *Anat. Rec.*, 114, 383, (1952).

(19) Neuman, W. and Neuman, M.: Chemical Dynamics of Bone Mineral, Univ. of Chicago Press, 1958.

the surface electrical fields. However, as Glimcher (2) has pointed out this excess water is many times greater than is usually considered possible for surfaces to bind as a result of electric field effects. Furthermore, Neuman and Neuman are unable to explain how the substitution of  $\text{H}_3\text{O}^+$  (ionic radius 1.4 Å) for  $\text{Ca}^{++}$  (ionic radius 1 Å) in maximum of 20% of the calcium positions can occur with no change in the XRD pattern. Posner, (20) says that such a substitution would result in an altered pattern. He holds that there is an absence of calcium ions from structural positions within the lattice with subsequent inclusion of protons to maintain electrical neutrality. Hendricks and Hill (21) interpret their chemical evidence to show that the low Ca/P of bone mineral is the result of excess phosphate adsorbed onto the surface of the tiny crystals. However, this has not been verified directly, and there are a number of theoretical objections to it (20).

A further mechanism relevant to the aberrant Ca/P of bone mineral was suggested by Glimcher (2) who pointed out that for crystals as small as those of bone mineral in which 65% of the unit cells are on the surface, the actual stoichiometry will be determined by the planes in which crystal growth ceases. Since one does not expect that all crystals are perfectly formed there is an inherent lack of stoichiometry independent of any substitution, absorption, unsubstituted defects, etc.

A proposal concerning the nature of bone mineral that has

- 
- (20) Posner, A. and Perloff, A.: J. Res. Nat. Bureau Stand., 58, 279, (1957).  
(21) Hendricks, S. and Hill, W.: Proc. Nat. Acad. Sci., 36, 731, (1950).

gained some support is that bone mineral is not HA but rather octocalcium phosphate (OCP),  $\text{Ca}_4\text{H}(\text{PO}_4)_3 \cdot 3\text{H}_2\text{O}$ , or, alternatively, that bone mineral in its initial stage of formation is OCP and is converted to HA in situ (22). The original discussion of the relation of OCP to HA is that of Arnold (23) who described OCP as a two dimensional sheet of HA, the sheets being held together by water molecules. Brown, et. al. (22) have found that the OCP structure is more complicated and have pointed out that while closely related OCP and HA are not isostructural accounting for the slightly different XRD patterns seen between the two materials. They find that when the hydrate water is eliminated by heating the XRD pattern becomes that of HA. The same result is found by Glimcher (2) by electron diffraction. If bone mineral possesses the layer-type structure of OCP ( $\text{Ca}/\text{P} = 1.34$ ) or is intermediate between OCP and HA, both the water loss on heating and the low  $\text{Ca}/\text{P}$  could be understood. It is apparent however, that the question cannot be resolved by crystallographic methods owing to the similarity of HA and OCP and even more so of lamellar mixtures of these two salts (24).

There have been a number of attempts to devise models of bone mineral which incorporate the impurities, particularly carbonate, directly into the crystalline structure. Such attempts have been motivated by the fact that there exist naturally occurring mineral apatites such as francolite, a fluorapatite which contains 3%

(22) Brown, W., Lehr, J., Smith, J., and Frazier, A.: J. Am. Chem. Soc., 79, 5318, (1957).

(23) Arnold, P.: Trans. Faraday Soc., 46, 1061, (1950).

(24) Brown, W., Lehr, J., Smith, J., and Frazier, A.: Nature 196, 1050, (1962).

carbonate. It was initially thought that the carbonate was in a lattice position and the analogy was made that bone mineral was a carbonate apatite. However, later work showed that francolite was a multiphase system and not a continuous lattice incorporating carbonate (11). In addition, there is some chemical evidence indicating that in bone mineral the carbonate is absorbed onto the surface (25). The prevalent view appears to be that of Neuman and Neuman (19) who point out that the extremely small size of bone mineral crystals and the resulting large surface area ( $\sim 100 \text{ m}^2/\text{g}$ ) provide ample surface for the adsorption of various foreign ions including carbonate. It is a well known fact that finely divided synthetic HA mirror their ionic environment. Thus, in their view the impurities are a "passive physiochemical consequence" of their presence in body fluids.

Finally, summarizing the evidence to 1958, Neuman and Neuman (19) report that there is no convincing evidence to indicate the presence of an amorphous phase associated with bone mineral. Recently, however, the presence of large amounts of amorphous calcium phosphate have been reported by Harper and Posner (26) in various animal bones. They used an X-ray technique and found the amorphous content to be more than 40%. By infrared analysis Termine and Posner (27) concluded that amorphous calcium phosphate was a major constituent of rat bone. The amorphous content varied, depending on age, from 69.5% to 35.5%.

---

(25) Brasseur, H., Dallemagne, M. and Melon, J.: *Nature*, 157, 453, (1946).

(26) Harper, R. and Posner, A.: *Proc. Soc. Exp. Bio. Med.*, 122 937, (1966).

(27) Termine, J. and Posner, A.: *Science*, 153, 1523, (1966).

In summary, bone mineral may be regarded as an impure HA or closely related crystalline compound (OCP). The crystals average about 200 A in the longest dimension and contain a considerable amount of amorphous calcium phosphate. The extremely large and chemically active specific surface of bone mineral results in a variety of ionic substitutions and in the adsorption of foreign ions. It also binds large amounts of water on the surface and may incorporate water or hydronium ions directly into the crystalline lattice.

## II. DIELECTRIC CONSTANT AND BOUND WATER OF BONE

## Introduction

Water is a major constituent of all biological organisms, comprising anywhere from 50% to 80% of the total weight of living plants and animals. In some cases, for instance the cerebrospinal fluid or blood plasma, it is present in bulk form and therefore exhibits the physical properties of ordinary water, due regard being taken for the presence of the solute. Such water is generally termed "free", the implication being that its dynamics in the organism can be understood by studying a model in vitro system in which the effect of the membrane enclosure need not be considered. In other cases however, water is not free but is complexed with organic material such as protein, cell protoplasm, DNA, and various membranes. The complexed or "bound" water is generally held to have an ice-like structure resulting from its interaction with the biological substrate. It has been increasingly recognized in recent years that many physical properties of biological materials cannot be understood adequately without consideration of their bound water. Conversely, many of the properties of bound water are markedly different from the corresponding properties of free water.

Interest in bound water of biological systems stems from the belief that it may have an important functional role. For instance, using nuclear magnetic resonance, Berendsen (1) has

---

(1) Berendsen, H.: J. Chem. Phys., 36, 3297, (1962).

found that water in the protein collagen forms chain-like structures, and that an integral number of water molecules can be fitted to the repeating unit in the Rich-Crick model of that protein.

Thus, he suggests that water may stabilize the collagen molecule by forming parallel chains that hydrogen bond extensively with the protein. The same role for water has been proposed in DNA.

It is now recognized that water may be an important factor in the stability of the helical double-strand structure (2). Rosenberg (3) has found that the electrical conductivity of hemoglobin varies over nine orders of magnitude depending on its water content.

In the case of water bound to cell membranes, Ling (4) has proposed that the hydrated structure may have the property of excluding or inhibiting the diffusion of some solutes such as ions and sugars, and hence it would play an important role in body metabolism. Lastly, crosslinking of the peptide chains of collagen has frequently been postulated to occur in aging (5), and the process may proceed at least in part by means of the systematic removal of bound water.

One expects that water molecules in the immediate vicinity of the substrate will be most strongly bound, and that succeeding layers will be less strongly held and will have physical properties approaching those of free water. Thus, an important parameter in addition to the total amount of bound water, is the amount having an energy of interaction with the substrate of more than a

---

(2) Yevdokimova, Y., Varshavskii, Y.: *Biofizika*, 11, No. 1, 7, (1966).

(3) Rosenberg, B.: *J. Chem. Phys.*, 36, 816, (1962).

(4) Ling, G.: *Fed. Proc., Fed. Am. Soc. Ex. Bio.*, 25, No. 3, Part 1, 958, (1966).

(5) LaBella, F. and Paul, G.: *J. Gerontol.*, 20, 54, (1965).

characteristic value  $E_0$ . Commonly, this part of the total bound water is called the "primary adsorbed water" and corresponds to the first adsorbed layer. It is the determination of the amount of primary adsorbed water in bone with which we will be concerned.

Determinations of the amount of primary adsorbed water present in purified proteins have been made by analysis of weight-hydration curves (6), and by dielectric constant studies (7). However, comparable measurements have not been made for bone, or in fact any organized tissue. Newly forming bone contains as much as 90% water while mature cortical bone has a water content as low as 3% (8), but the fraction of this water that exists in the primary bound state has not been reported. A determination of this quantity is of interest for several reasons. First, knowledge of the amount of primary bound water may give information concerning the amount associated with each of the two major constituents of bone, collagen and apatite. This in turn is an important factor in the study of the internal chemistry of these materials. The etiology of a vast number of osteogenic diseases is unknown and the idea that the degree of hydration may be of prominent importance is being seriously considered. A necessary first step is the characterization of the water content of normal bone. Secondly, water has an important effect on the electrical properties of bone (9, 10). Its electrical conductivity for instance, shows a non-linear dependence on humidity. A determination

- 
- (6) Bull, H.: J. Amer. Chem. Soc., 66, 1499, (1944).  
(7) Rosen, D.: Trans. Faraday Soc., 59, 2178, (1963).  
(8) Frost, H.: Bone Remodelling Dynamics, Thomas Co., 1963.  
(9) Bassett, C. and Becker, R.: Science, 137, 1063, (1962).  
(10) Becker, R., Bassett, C. and Bachman, C.: Bone Biodynamics, Frost, H. (ed.), Little, Brown, & Co., 1964.

of the primary bound water was necessary in order to ensure that future electrical measurements were made on samples which possessed a standard complement of bound water.

The purpose of the present work was to determine whether different physical states of water adsorbed on bone from the vapor phase could be detected and measured. Adsorption from the vapor phase rather than immersion in water or simulated physiological fluids was chosen because hydration by adsorption can be produced and measured systematically. This is in contrast to the all-or-none effect produced by immersion. In view of the highly polar nature of the water molecule, and the fact that its ability to orient in an alternating electric field should depend on the strength of its interactions with the substrate, the property chosen for study was the complex dielectric constant  $\epsilon$ .

In many cases, the dielectric behavior of water adsorbed on organic and inorganic adsorbents alters sharply at a particular amount of the adsorbate. Such is the case for water absorbed on protein powders (7), gamma alumina (11), silica gel (12), and magnesium hydroxide (13). For some adsorbents, alteration of the dielectric behavior can be interpreted in terms of the Brunauer-Emmett-Teller (BET) (14) theory of multilayer adsorption. The BET theory predicts that adsorption of water vapor (or any gas) onto a solid substrate at constant temperature is governed by:

$$w = \frac{w_m c p}{(p_0 - p) [1 + (c - 1) (p/p_0)]}$$

- (11) Balwin, M. and Morrow, J.: J. Chem. Phys., 36, 1591, (1962).  
 (12) Kurosaki, S.: J. Phys. Chem., 58, 320, (1954).  
 (13) Nelson, S., Newman, A., Tomlinson, T., and Sutton, L.:  
 Trans. Faraday Soc., 55, 2186, (1959).  
 (14) Brunauer, S., Emmett, P., and Teller, E.: J. Amer. Chem.  
 Soc., 60, 309, (1938).

$p$  = gas pressure

$p_0$  = saturation gas pressure

$w$  = total weight of gas adsorbed

$w_m$  = weight of gas adsorbed when the entire adsorbent surface is covered with a unimolecular layer. [BET monolayer].

$c$  = constant, related to heat of adsorption

The equation may be rewritten as:

$$\frac{p}{w(p_0-p)} = \frac{1}{w_m c} + \frac{c-1}{w_m c} \frac{p}{p_0}$$

A plot of  $p/w(p_0-p)$  against  $p/p_0$  should give a straight line whose intercept is  $1/w_m c$  and whose slope is  $(c-1)/w_m c$  and thus two constants,  $c$ , and  $w_m$ , can be determined. The dielectric behavior of these materials (11, 12, 13) undergoes a marked alteration when the BET monolayer is completed. Thus, the weight of condensed vapor in the monolayer may be determined from either a series of dielectric constant measurements or from the adsorption isotherm. However, for proteins or heterogeneous systems such as calcified tissue, a variation of the binding energy of different sites (i.e. different  $c$ 's) may cause adsorption on these materials to depart from BET-type behavior (7). In this case, the primary bound water of the system cannot be determined by an analysis of the adsorption isotherm; but it can be determined by dielectric constant measurements.

Since the measured dielectric constant of a hydrated system

receives a contribution from water which depends on the degree to which the water is structured or bound, its determination simplifies the study of adsorbed water by grouping together those water molecules which are in the same physical state. In the present work, both the dielectric constant and the amount of water adsorbed have been measured explicitly as a function of relative humidity (RH).

### Experimental

#### Sample Preparation:

Human bone samples were obtained from fresh lower-extremity amputation specimens (femur, tibia). All samples were from clinically normal bone, the amputations being necessitated by mechanical or traumatic considerations. The periosteum, marrow and all cancellous bone were removed, as was a thin layer of subperiosteal and subendosteal bone. The samples were cut into regular geometrical shapes to facilitate measurement of the dielectric constant. In the preliminary preparation, the samples were cut slowly, by hand, to avoid denaturation of the protein component. The final polishing was done with a graded series of abrasive papers. The resulting samples had thickness to area ratios ( $t/a$ ) varying from  $0.055 \text{ cm}^{-1}$  to  $0.114 \text{ cm}^{-1}$ . Care was taken to ensure that the samples were rectangular and as free as possible from surface defects. At no time were they immersed in solution or treated with chemicals. The largest dimension of all

samples was along the original long axis of the bone, and all dielectric measurements reported were made at right angles to this axis.

Saturated salt solutions (15) giving the desired RH were used to control the bone water content. Samples were supported above the salt solutions by thin gauze sheets, and were permitted to reach equilibrium with the controlled atmosphere. (See following two sections).

Apparatus:

Measurements of  $\epsilon'$  and  $\epsilon''$ , the dielectric constant, and dielectric loss, were made at the frequencies 100 kc, 50 kc, 10 kc, and 1 kc, employing a General Radio type 716-C Capacitance Measuring Assembly, and a type 1690-A micrometer-driven dielectric sample cell. The cell was fitted with side plates especially fabricated to allow a determination of  $\epsilon'$  and  $\epsilon''$  for completely dry bone in a controlled atmosphere (dry nitrogen). The increase in capacitance and conductance across the terminals of the sample cell due to the insertion of the sample were measured.  $\epsilon'$  and  $\epsilon''$  were then calculated using cell constants, due allowance being made for the fraction of the volume of the cell not occupied by the sample. (See Appendix A). Individual capacitance measurements could be made to an accuracy of 0.25%. The resulting relative error of the computed dielectric constants varied with the t/a of the samples but was generally less than 3%.  $\epsilon''$  was

---

(15) Lange, N.: Handbook of Chemistry, 1949, pg. 1432.

measured to 2% or  $\pm 0.07$  whichever is greater. Conductivity measurements were made using a Hewlett-Packard model 425 AR Microammeter.

The RH maintained by the saturated salt solutions (range 12% - 82%) were measured to an accuracy of  $\pm 1.5\%$  by means of a HygroDynamics Inc. wide-range humidity sensing element No. 15-1810, and matching Electric Hygrometer Indicator No. 15-3001. An airtight humidity chamber was constructed for this purpose from Plexiglas and fitted with a threaded aluminum cap in which the sensing element was mounted. The ratio of the volume of the chamber to the surface area of the solution was about 50 cm. The RH maintained by the solutions in the room temperature interval  $21^{\circ}\text{C} \pm 2^{\circ}\text{C}$  together with the Handbook Values (15) for  $20^{\circ}\text{C}$  are given in Figure 6. During the experiment the room temperature was maintained at  $21^{\circ}\text{C} \pm 2^{\circ}\text{C}$  and the room RH generally below 30%.

Procedure:

The general procedure was as follows: the prepared sample was first vacuum dried at a pressure of approximately 50 microns and its dry weight, volume, and dielectric constant determined. It was then equilibrated with the atmospheres maintained by the saturated salt solutions. When equilibrium was attained at a particular RH the sample was removed and the dielectric and weight measurements were made in an average time of eight minutes. The sample was then transferred to the next highest RH. In order to

avoid hysteresis effects, all measurements on a given sample began at the lowest attainable RH (12%) and proceeded stepwise through to the highest RH (82%). Each sample was treated as a specific entity and all measurements were made directly on the sample for which data are reported. Thus, for each sample, the results were a series of curves,  $\epsilon'$  versus frequency,  $\epsilon''$  versus frequency, with hydration or water content as a parameter. Also, the dependence of equilibrium water content on RH (adsorption isotherm) was determined for each sample.

In view of the method used, two restrictions were imposed:

- (a) dielectric readings were taken at four frequencies only,
- (b) relative humidities above 82% were not employed. The former arises because the time required for additional frequency measurements would be prohibitive. For a total elapsed time of measurement greater than approximately eight minutes, the samples begin exchanging with the room water vapor. The weight and dielectric constant then become functions of time. The latter restriction results from the very rapid exchange that takes place between samples that are equilibrated at RH above 82% and then exposed to the room RH of about 30%. In this case weight changes are seen almost immediately and accurate measurements could not be taken. Both restrictions are necessary in order that the assumption of equilibrium during the measurement be a reasonable one.

There is an inherent ambiguity in any definition of "dry"

bone and as a result there are a number of competing criteria. One may, for instance, heat to constant weight at 100°C and define bone so treated as "dry". However, there are no assurances that the resulting material will have the same physical, chemical or electrical properties as bone dried in another manner. Indeed, there is some evidence to the contrary. Also, the protein fraction of bone is known to undergo denaturation at about 64°C, and this may have an important effect on the adsorption properties of bone. In view of these considerations, dry bone is defined for the purposes of this study as bone in equilibrium with a water-free atmosphere at 50 microns pressure and room temperature. This procedure is believed to result in a minimum amount of irreversible change of the sample. In practice, reproducible measurements of the dielectric constant are obtained over several dehydration-hydration cycles. For the sample sizes of interest, it is found by weight monitoring that two months are required for the drying process. After this time no weight change is seen to  $\pm 0.3$  mg. All samples for which data are reported were vacuum dried a minimum of two months. It should be recognized that the criterion adopted for "dry" bone is a definition and the results of the experiment are not independent of it. (See Appendix C).

The question arises as to how long is required to establish equilibrium at a given RH. In order to answer this the following experiment was performed. Two samples were vacuum dried, and then

placed in separate chambers that had been modified to allow conductivity measurements while the sample was being hydrated. The RH in one chamber was maintained at 50% and in the other at 98%. The direct current conductivity was monitored periodically for two weeks and as can be seen from Figure 7, equilibrium was attained for the worst case after approximately one week. The same results were obtained in another experiment in which the weight of the sample was monitored. In view of these results, and since in the actual experiment no sample was subjected to a RH change of more than about 12%, one week was allowed for equilibrium to be attained at each RH before any measurements were taken.

#### Results

Typical results for the dielectric constant are given in Figure 8. As can be seen, the  $\epsilon'$  versus  $\log f$  plots are sensitive to water content. In all cases, for a given hydration,  $h$  (mg of water per gram of dry bone),  $\epsilon'$  decreased continuously with increasing frequency. When the results are plotted as in Figure 9, with frequency as the parameter, the points are found to lie reasonably well along two straight line segments having different slopes. After excluding the point corresponding to  $h=39.8$ , a best fit straight line can be calculated for each line segment. The intercept of the lower line gives an extrapolated value of the dielectric constant of completely dry bone. The intersection of the two lines defines a quantity  $h_c$ , the "critical hydration" of bone.

Results for  $\epsilon''$ , the dielectric loss, are given on Figure 10. Again the dependence on water content is evident. The large resistance of low water-content bone causes the corresponding values of  $\epsilon''$  to be of the same order as the experimental error. For higher water contents, no dielectric loss maxima were seen, even for samples on which more detailed frequency measurements were taken.

When  $\epsilon''$  is plotted against hydration, the points again fall along two straight line segments whose intersection similarly defines  $h_c$  (Fig. 11). The qualitative behavior of both  $\epsilon''$  and  $\epsilon'$  versus  $h$  is the same, and since the values for the latter curves are more accurately known, they have been used to determine the magnitude of  $h_c$ .

The value of  $h_c$  for the sample discussed (Sample #1) together with relevant data for the other samples examined is given in Figure 12. In each case  $h_c$  is determined by the intersection of the two line segments at 100 kc, 10 kc, and 1 kc and is averaged over the three results. The line segments themselves were obtained from a linear least squares analyses of the data points; the data points in the transition region and at  $h = 0$  were excluded. The density given in Figure 12 was determined simply from measurements of the linear dimensions of the sample. It takes no account of the various kinds of spaces or cavities in bone and is only a measure of the relative compactness of the various samples.

The average adsorption isotherm for bone is given in Figure 13. It is seen to be linear over a rather wide range of relative humidities, in contrast to the S-shaped curves usually obtained for adsorption on homogeneous substances. For values of the RH above 82%, the curve is very steep and accurate measurements could not be taken.

An increase in the linear dimensions of the samples with increasing hydrations was observed. Relative to the dimensions at zero water content, the average increase for bone in equilibrium with a RH of 82% was 2.5% for dimensions at right angles to the collagen fibers, and 0.5% along the fibers.

#### Discussion

The literature contains many references to what are called the "bound water" and "free water" compartments of bone. The bound water compartment is generally thought to be of a relatively fixed size and to contain water which is ordered or structured by individual (primary) binding sites in the tissue. The free water compartment contains the less strongly held water found in bone. Our experiment clearly indicates that the equilibrium water content of bone is determined solely by the RH of the atmosphere with which it is in equilibrium (c.f. Fig. 13), as indeed is the case for all other hygroscopic materials which have been reported.

The experimentally determined quantity,  $h_c$ , may be interpreted as the primary bound water of bone (7, 11-13). That is, the amount

of water necessary to occupy the primary adsorption sites in bone. In this connection the following model has previously been proposed to account for results similar to the present ones (7, 11-13): for low equilibrium water contents the adsorbed water is structured or irrotationally bound so that it is essentially able to make only an electronic or molecular contribution to the measured dielectric constant of the system. That is, there is a minimal contribution from reorientation of the water dipole moments in the electric field. For progressively higher water contents, the adsorbed water is present in the second and subsequent layers and is less strongly held, i.e. is relatively "free" and therefore able to make a significant orientational contribution, resulting in the steep rise seen in Figure 9;  $h_c$  is then the dividing point between the two regions.

There is the possibility that the observed dielectric dispersion contains a contribution from a form of interfacial polarization. For instance, at high water contents surface ions from bone mineral may acquire a certain local mobility in the electric field and thus produce a Maxwell-Wagner form of dispersion which could account in part for the high dielectric constants seen at high water contents. Such a mechanism would however, be expected to present only at the higher RH where capillary condensation occurs, a phenomena in which water condenses in bulk form in capillaries, microscopic cracks, and vascular spaces. In the present experiment, no evidence was seen

that would indicate water was present in bulk form in samples in equilibrium with RH of 80% or less. Above 80% bulk condensation does occur as evidenced by glistening of the sample surface when viewed under the light microscope. In any event, whether the dominant mechanism responsible for the steep rise seen in Figure 9 is (a) orientational, resulting from secondary adsorbed layers or (b) interfacial polarization, resulting from bulk condensation of water, it appears possible to identify  $h_c$  with the amount of water required to fill the primary adsorption sites in bone (PASB).

The results give some information concerning the nature of the PASB. It is thought that adsorption on proteins involves an interaction between water molecules and local dipoles along the protein molecule and that adsorption on the mineral hydroxyapatite results from the electric field asymmetry at the surface of the individual crystals (producing the "hydration shell"). Thus, adsorption in bone may correspond to a superposition of the two effects. Indeed, on the basis of this assumption good agreement with data in the literature is obtained as follows: adsorption isotherms for synthetic hydroxyapatite (16) and hide collagen (6) have previously been reported. Both isotherms were fitted to a BET-type equation resulting in values, for the amount of water necessary to occupy the primary adsorption sites,  $w_m$ , of 17.6 mg/g for hydroxyapatite and 95.2 mg/g for collagen. If, for simplicity, a gram of bone is assumed to consist of 65% apatite and 35% collagen by weight, then

(16) Neuman, W., Toribara, T., and Mulryan, B.: J. Amer. Chem. Soc., 75, 4239, (1953).

one arrives at the value  $(0.65)(17.6) + (0.35)(95.2) = 44.8$  for the water necessary to occupy the PASB, as compared with the experimentally determined range of (37-48). Furthermore, at the conclusion of the experiment, the samples were ashed at  $500^{\circ}\text{C}$  for twenty-four hours and the per cent mineral content was found to be  $68.5\% \pm 1.1\%$ . It corresponds to a value for the PASB of  $42 \pm 1$  which is in even better agreement with the experimental results. Hence, it appears that adsorption of water by bone may be a superposition of adsorption by collagen and apatite separately with collagen playing the dominant role in terms of amount adsorbed. Such a conclusion is surprising in view of the structural organization of bone. It would mean that whatever the nature of the binding between apatite and collagen in bone, it is such that the primary adsorption sites of both have direct access to the vapor phase and are not, for instance, sequestered, or involved in chemical binding between one another.

Even though, (a) adsorption on collagen and apatite separately has been found to obey a BET-type equation, and, (b) the results reported here are interpretable in terms of the BET constants for collagen and apatite, this does not necessarily imply that adsorption on bone follows a BET-type equation. It may or it may not, and the adsorption isotherm given in Figure 13 is not sufficiently detailed to answer the question. It does not contain a sufficient number of points in the RH range of 5% to 35%, the optimum range for deter-

mining the BET constants. A system of any two BET adsorbers will, in general, not be a BET adsorber. The exception is when,  $c$ , the BET constant related to the heat of adsorption, is the same for each adsorber. If the adsorption isotherm of bone is found to fit a BET-type equation, then the value of the bound water that is thus determined would be expected to agree with the value of  $h_c$  reported here. If adsorption in bone is found to be non-BET, then one may conclude only that the heats of adsorption on collagen and apatite are different and no definitive statement concerning the amount of bound water can be made.

Reference to Figure 12 shows that the measured values of the dielectric constant of dry bone are slightly but consistently larger than the extrapolated values. A possible explanation is that bone, vacuum dried in the manner previously described, contains residual water. The amount of water, having the dielectric properties of bulk water, that is necessary to produce the observed increment is not large ( $\sim 1$  mg/cc). However, for strongly bound water unable to make a significant dipolar contribution, the amount required to account for the difference would be greater. Thus on the basis of this experiment it is not possible to relate the observed difference to a specific amount of residual water. Alternatively, extrapolation to zero water content may not be valid. That is, the portion of the  $\epsilon'$  versus  $h$  curve with hydrations in the range 0 to 8 mg-H<sub>2</sub>O/g-bone may define a third linear line segment (and a second critical

hydration) as for instance has been found for water adsorbed on silica gel (12). More data in the low hydration region are needed in order to settle the point.

As can be seen in Figure 9, the slope of the line segment joining the points at the higher hydrations increases as the frequency of measurement decreases. The effect can be interpreted as being due to the increased ability of water on the secondary adsorbed layers to make an orientational contribution as the frequency is lowered. It can be seen that in an effort to distinguish experimentally between different states of adsorbed water, the frequency of measurement can be an important parameter, and this was in fact the reason the experiment was done at a number of frequencies. For a frequency range either higher or lower than the one chosen, a change in dielectric properties would probably not have been observed.

The dielectric loss (Fig. 10) likely contains contributions from all three of the possible mechanisms, Debye-type relaxation, interfacial polarization and Joule heating losses. With the exception of several attempts to find a maximum in  $\epsilon''$  with frequency which would be indicative of Debye relaxation, the dielectric loss was not intensively studied. If a maximum does exist, it is at frequencies greater than 100 kc. It is pointed out however, that all three mechanisms are consistent with both the change in  $\epsilon''$  seen at  $\sim 48$  mg-H<sub>2</sub>O/g-bone, and with the increasing slope seen with

decreasing frequency.

In conclusion, the results obtained indicate that water adsorbed on bone exists in at least two separate states, one more strongly bound to the underlying matrix than the other. The amount of water that is in the primary bound state varies from 37 to 48 mg-H<sub>2</sub>O/g-bone. This range is in good agreement with the amount of water known to be present in the primary bound state in collagen and hydroxyapatite.

Appendix A - Equations Used to Determine  
Dielectric Constant and Dielectric Loss

In the Schering Bridge employed (17) two capacitors are adjusted to balance independently the resistive and reactive components of the current. If the capacitor being measured is represented by a pure capacitance  $C_s$  in series with a pure resistance  $R_s$  then at null the bridge is direct reading in  $C_s$  and  $D$  where  $D$  is the dissipation factor defined as  $D = \omega R_s C_s$ , and  $\omega$  is the angular frequency. Since the resistance of a capacitor is in parallel with its capacitance, it is the parallel values  $C_p$  and  $R_p$  that are needed. These quantities are related as follows:

$$C_p = \frac{C_s}{1 + D^2}$$

$$R_p = \frac{1 + D^2}{D\omega C_s}$$

If after the insertion of the sample  $C_s$  is the series capacitance  $C_p$  the parallel capacitance and  $D$  the dissipation factor, then the change in parallel capacitance is:

$$\Delta C_p = \frac{C_s}{1 + D^2} - C_0$$

Where  $C_0$  is the capacitance of the empty capacitor. If the sample has area  $A_x$  and thickness  $t$  then the resistivity of the sample in terms of measured quantities is:

$$\rho = \frac{1 + D^2}{D\omega C_s} \left[ \frac{A_x}{t} \right]$$

(17) Marton, L.: Methods of Experimental Physics, 6, Part B, Academic Press, 1959, pg. 9.

$\epsilon'$  and  $\epsilon''$  are defined as (18):

$$\epsilon' = \frac{C_p}{C_o}$$

$$\epsilon'' = \frac{1}{\omega R_p C_o} = \frac{1}{\omega C_o \rho \frac{t}{A}}$$

Where A is the area of the capacitor plates and t is their separation. Substituting for  $\rho$  we have for  $\epsilon''$ :

$$\epsilon'' = \frac{A}{A_x} \frac{C_s}{C_o} \frac{D}{1 + D^2} \quad [1]$$

For  $\epsilon'$ , since the sample does not fill the entire volume we have:

$$\frac{A - A_x}{4\pi t} + \frac{\epsilon' A_x}{4\pi t} = C_p$$

and

$$\frac{\epsilon' A_x}{4\pi t} - \frac{A_x}{4\pi t} = \Delta C_p$$

or

$$\epsilon' = \frac{4\pi t}{A_x} \Delta C_p + 1$$

Substituting in for  $\Delta C_p$  we obtain:

$$\epsilon' = \frac{4\pi t}{A_x} \left[ \frac{C_s}{1 + D^2} - C_o \right] + 1 \quad [2]$$

Equations [1] and [2] were used to calculate  $\epsilon'$  and  $\epsilon''$ .

### Appendix B - Results of an Experiment on Pathological Bone

During the course of this work, it became apparent that different physical states of adsorbed water could in fact be distinguished by dielectric measurements. As the experiment was repeated, the points in the  $\epsilon'$  versus  $h$  curves consistently fell along two straight line segments. Since the behavior of samples of normal bone had been established, an attempt was made to study the behavior of pathological bone under the same conditions. The particular pathology chosen was Giant Cell Tumor.

Giant Cell Tumor (19) is a neoplastic growth usually found in the medullary cavity of the tubular bones. The tumor is composed of a matrix of collagen fibers in which are imbedded multinucleated giant cells believed to be derived from osteoclasts. The growth of the tumor takes place at the expense of cortical bone which is resorbed so that in the region of the tumor, the average diameter of the medullary cavity is greater and the average wall thickness is less than in normal bone. The causative factors of the tumor, the mechanism by which bone is resorbed and the role of the giant cells are all unknown. In the present case, the growth had recurred several times in the region of the distal femur necessitating surgical removal of the limb. The sample examined was taken from an area approximately four inches distal to the tumor site. Histologically, bone in this area is normal. Whatever the factors involved in the tumor growth, they are believed to be

---

(19) Boyd, W.: Textbook of Pathology, Lea & Febiger, 1961.

localized to the region of the tumor.

The results for  $\epsilon'$  versus  $h$  are given in Figure 14 for frequencies of 100 kc, 10 kc, and 1 kc. As can be seen, the dielectric constant increased with hydration but in a rather random way. In contrast to all other samples examined, no discrete change in dielectric behavior with hydration was seen. As a result the critical hydration could not be defined. In addition, the dielectric constant at zero water content is approximately 9% greater than the average of the dry dielectric constant of the normal samples (c.f. Fig. 12). Since the sample was prepared and measured under the same conditions as all other samples and lacking any evidence to the contrary, it will be assumed that the erratic behavior of the  $\epsilon'$  versus  $h$  curve is due to the sample itself and not some unknown systematic error.

The results suggest that Giant Cell Tumor may be associated with a defect in the bone per se rather than with a defect in the region of the tumor. Suppose for instance, that there is a disturbance in the normal bound water of bone. Then, by affecting either the diffusion of solute ions, or the molecular bound water on the membranes of normal cells located in the medullary cavity this could conceivably result in cell aggregation and trigger the production of a defective form of collagen. Unable to incorporate into the bone matrix, the collagen would coalesce to form a stroma as is found in Giant Cell Tumor. The interior of the long bones

would provide an ideal incubator for the tumor. Bather, et. al. (20) have shown that for bound water below a certain level the carcinogenic capabilities of tumor cells are greatly increased, by virtue of the release of virus particles. Such a mechanism here could explain the malignancy that occurs in approximately 50% of the cases of Giant Cell Tumor.

The above speculations are consistent with the facts that histologically and spectrographically\*, bone distal to the tumor site appears normal. They are based on the erratic dielectric behavior of one sample of pathological bone as compared with the normal samples.

---

\* Spectrographic comparison of normal and diseased bone performed by Mr. J. Spadaro.

(20) Bather, R., Webb, S., and Cunningham, T.: Nature, 207, 30, (1965).

## Appendix C - Method of Drying Employed

In reviewing this work, one referee has pointed out that the criterion adopted for dry bone is not that normally employed. He suggested as an alternative that the samples be heated to say 100°C, and the weight thus determined be defined as the dry weight. Because sample heating grades directly into sample destruction, the vacuum drying method previously described was employed. The validity of the method was tested at the conclusion of the experiment in the following manner. The samples were again vacuum dried and then heated to 100°C and the weight loss from vacuum to 100°C was determined. The result was that the samples showed an average weight loss of  $34.4 \pm 4.0$  mg/g\*. The question then is whether this weight loss represents an amount of water tightly held by the substrate and not removed by vacuum drying to the pressure employed, or a weight loss which is a direct result of a partial decomposition of the substrate? In the former case, the results reported here for the value of  $h_c$  would be in error by about the amount of weight loss seen, while the latter case would indicate that an irreversible change taken place during heating and hence would support the criterion for dry bone adopted here and the value of  $h_c$  thus determined.

The question was resolved in the following manner: the 100°C weight is 34.4 mg/g below the vacuum weight and the 31% RH weight (i.e. weight of samples in equilibrium with RH of 31%) is found to

\* Tolorances here and in the numbers that follow represent one standard deviation. No distinction is made between mg/g-vacuum dried bone, and mg/g-100°C heated bone, since the error involved is quite small.

be  $31.9 \pm 5.4$  mg/g above the vacuum weight. If the weight loss of 34.4 mg/g is due to the dehydration of adsorbed water and if heating to  $100^{\circ}\text{C}$  is a reversible procedure then the weight gain of samples first heated to  $100^{\circ}\text{C}$  and then equilibrated with an RH of 31% should be in the vicinity of 66 mg/g.

Such an experiment was carried out on a set of four samples with the result that the average weight regain was  $40.7 \pm 11.4$  mg/g which is approximately the weight gain seen from vacuum to 31% and is far less than would be expected under the above assumption. The results indicate that heating to  $100^{\circ}\text{C}$  does cause irreversible damage and they show that the weight loss seen between vacuum and  $100^{\circ}\text{C}$  is principally a result of the partial decomposition of the substrate and not the liberation of tightly held water. Thus, the numerical value for primary bound water given here is not in substantial error due to water remaining after vacuum drying.

### III. ELECTRON PARAMAGNETIC RESONANCE STUDY OF BONE AND ITS MAJOR COMPONENTS

#### Introduction

While the literature is replete with reports of Electron Paramagnetic Resonance (EPR) studies on irradiated biological materials, one finds only scanty references to work on non-irradiated calcified tissue. Slager and Zucker (1) found a singlet at  $g=2.0$  in X-irradiated bone prepared for use in bone banks, and Cole and Silver (2) reported the presence of trapped hydrogen atoms in a single irradiated deciduous tooth. Both investigators reported no resonances in the non-irradiated materials which had been employed as controls. However, the presence of complex EPR signals in X-irradiated rat femur has been reported by Swartz (3) and in X-irradiated human femur by Termine, et. al. (4). In both cases, the non-irradiated controls exhibited a weak singlet at  $g=2.0$ . The presence of anisotropic resonances in whole bone samples of non-irradiated frog and human tibia and of an isotropic singlet at  $g=2.0$  has been reported by Becker (5). With one exception (2), the magnetic species responsible for the observed resonances has not been identified. Commoner (6) has stated that the resonances in whole bone (5) are most likely due to its mineral content, however no EPR studies of bone mineral have been reported.

In the case of collagen, which forms the protein matrix of bone, a singlet at  $g=2.0$  has been reported in UV-irradiated

- (1) Slager, V., and Zucker, M.: *Transplant. Bull.*, 30, 146, (1962).
- (2) Cole, T., and Silver, A.: *Nature*, 200, 700, (1963).
- (3) Swartz, H.: *Radiation Res.*, 24, 579, (1965).
- (4) Termine, J., Pullman, I., and Posner, A.: *Arch. Biochem. Biophys.*, 122, 318, (1967).
- (5) Becker, R.: *Nature*, 199, 1304, (1963).

collagen (7) and a doublet in X-irradiated collagen (8). No resonances have been reported in non-irradiated collagen.

An EPR study of bone was undertaken as part of a comprehensive study of the physical properties of this material. In particular, a growth control system has been postulated to govern at least one form of bone growth (9, 10). In the proposed control system, collagen and apatite are assumed to be semiconductors with a large band gap. There exists the possibility of detecting unpaired electrons as paramagnetic donor states and thereby obtaining confirmatory evidence for the proposed theory.

Collagen and apatite were studied individually because of their importance in the structure of bone. By comparing the results from bone with those from collagen and apatite, it was hoped that information could be obtained concerning the organization of bone on the molecular level.

#### Preparation

Procurement of bone was as described in Part II. The basic samples were prepared by removing the marrow, periosteum, and all cancellous bone from selected specimens of human femur and tibia. They were then stored in air (Petri dishes) under normal laboratory conditions of temperature, humidity and illumination until examined. Whole bone samples were prepared by hand sawing the cortical bone into 2 x 2 x 20 mm sections and had a final weight of about 200 mg. Bone powder was prepared by slowly scraping samples of cortical bone

- 
- (6) Commoner, B.: In Proc. Conf. Aseptic Necrosis of the Femoral Head, St. Louis, Mo., 1964.  
(7) Forbes, W. and Sullivan, P.: *Biochim. Biophys. Acta*, 120, 222, (1966).  
(8) Patten, R. and Gordy, N.: *Rad. Res.*, 22, 29, (1964).  
(9) Becker, R., Bassett, C. and Bachman, C.: Bone Biodynamics, Frost, H. (ed.), Little, Brown, & Co., 1964.

with glass microscope slides while the sample was held in a vise fitted with teflon jaws. The result was a fine powder uncontaminated by metallic fragments. The final weight of bone powder samples was 100 mg.

Collagen may be extracted from bone by incubating bone samples in a 5% formic acid solution; however, the reaction proceeds very slowly and in addition, does not remove all of the inorganic mineral. In this work, tendon which is about 95% collagen has been studied as a prototype of bone collagen. Clinically normal human peroneus longus tendon was obtained during surgery, its removal having been necessitated by traumatic or mechanical considerations. After removal, it was stored in air (Petri dishes) under normal laboratory conditions. Tendon, which immediately after removal from the body is soft and pliable, becomes hard and rigid when dry and its residual water content is within the limits set by EPR sensitivity considerations. Samples were prepared from dry tendon by cutting lengths along the fiber direction and placing in narrow bore (3 mm) quartz tubes. The final sample weight was usually about 75 mg. Dog, chicken, frog, and rat tail tendon were obtained immediately after the death of the respective laboratory animal. Bovine tendon was commercially purchased (Swartz Biochemical Co.). The animal tendons were stored and prepared in the same manner as human tendon.

Bone mineral was extracted by the standard procedure; refluxing with ethylenediamine vapor (11). In this method a concentrated

---

(10) Becker, R. and Brown, F.: Nature, 200, 700, (1965).

(11) Williams, J. and Irvine, J.: Science, 119, 771, (1954).

solution of ethylenediamine is heated and the resulting vapor is condensed and caused to fall on the samples where it dissolves the organic matrix. The solvent condenses continuously, and periodically the solvent plus dissolved matrix is flushed from the area of the samples to the reservoir from which the pure vapor originates. The process is continued for seventy-two hours. After refluxing, the samples were washed twenty-four hours in pure (distilled-deionized) water in order to remove the solvent.

A Varian X-band spectrometer V-4502-02 and six inch current-regulated magnet were used. During the course of the experiments, a nine inch field-regulated magnet was substituted for the six inch magnet. The field was modulated at 100 kc and the resonance signal was phase detected at this frequency resulting in a first derivative presentation. Variable temperature studies were done with a Varian V-4540 variable temperature accessory utilizing a constant flow of dry nitrogen at the desired temperature. When weak signals were being recorded, a Varian C-1024 time averaging computer was employed. g-values were calculated from a determination of the klystron frequency using a Hewlett-Packard wavemeter, type X532B. The first derivative of the absorption signal was recorded. The nominal sensitivity of the spectrometer is  $5 \times 10^{12}$  spins for a line having a width of ten gauss.

All chemicals used were Reagent grade. The atmosphere of the laboratory was temperature controlled ( $21^{\circ}\text{C} \pm 2^{\circ}\text{C}$ ) and humidity

controlled (< 30%).

## Results and Discussion

### Bone:

The EPR spectrum obtained from bone powder at room temperature is a relatively intense and sharp resonance at  $g=2.008 \pm 0.003$ . The line has a width of  $11 \pm 1$  gauss measured between peaks of the derivative and corresponds to a spin concentration of about  $1-4 \times 10^{16}$  spins/gram. As the microwave power is raised, the resonance saturates inhomogenously (12). Magnetic field scans from 100 gauss to 11,000 gauss revealed no other consistently present resonances. At  $114^\circ\text{K}$ , the results were identical with those at room temperature, except for an increase in signal intensity.

Bone powder was studied initially in an attempt to avoid any anisotropic effects that might be present. The results led us to expect from whole bone a resonance with a width of less than 11 gauss and a very slightly anisotropic g-value. Moreover, since the whole bone samples were twice the weight of the powder samples we expected an increase in signal amplitude. The results were just the opposite. The room temperature spectrum of whole bone is a singlet at  $g=2.008 \pm 0.003$ , again exhibiting a width of  $11 \pm 1$  gauss. No change in the g-value was seen as the angle between the fiber axis and the external magnetic field was varied. In addition, on an equal weight basis the intensity of the whole bone resonance is less than that of the powder by a factor (average) of 11.5. The

---

(12) Portis, A.: Phys. Rev., 91, 1071, (1953).

saturation behavior of the whole bone resonance is also different: it saturates homogeneously and shows a weak maximum at about 10 db below the nominal klystron power output (300 milliwatts). The whole bone resonance shows no appreciable change in amplitude as the temperature is lowered to 114°K. At this temperature the weak maximum at 10 db is still observed. Also at 114°K, in approximately half the whole bone samples examined, a barely resolved resonance is seen at about  $g=2.07$  with a line width of 150 gauss. No other resonances are seen with a consistency approaching 50%.

The literature contains a series of papers (13, 14, 15, 16, 17) describing the production of EPR spectra in a number of polymeric materials by the application of mechanical energy. The mechanical destruction is variously produced by filing or milling the polymer or by dispersing in a vibrating mill. Although the effect is poorly understood it is associated with the rupture of molecular chains and the formation of free radicals, some that are stable indefinitely. Usually materials treated in this manner exhibit intense EPR absorption in the vicinity of  $g=2.0$ . In particular, Ulbert (13) has reported intense asymmetric resonances from the protein keratin (similar in many respects to collagen) obtained by filing in atmospheres of air, and nitrogen with 7% oxygen. Abagyan and Butyagin (14) have observed intense EPR doublets from gelatin mechanically dispersed in air and in vacuo. To determine if such a mechanism was responsible for the resonance at  $g=2.008$  from bone

(13) Ulbert, L.: *Nature*, 195, 175, (1962).

(14) Abagyan, G. and Butyagin, P.: *Biofizika*, 9, No. 2, 180, (1964).

(15) Bresler, S., Zhurkov, S., Kasbekov, E., Saminskii, E. and Tomashevskii, E.: *J. Tech. Phys. U.S.S.R.*, 29, 358, (1959).

(16) Ulbert, K. and Butyagin, P.: *Doklady Akad. Nauk. S.S.S.R.*, 149, No. 5, 1194, (1963).

powder, it was dispersed in a vibrating mill for varying lengths of time. The results given in Figure 15 show the accumulation of free radicals as a function of the time of dispersion. In Figure 15, the ordinate is the amplitude of the derivative signal. The flat portion of the curve represents the attainment of equilibrium between the rates of free radical production and decay for a given (mechanical) energy input. The last point in Figure 15 corresponds to a spin density of about  $10^{17}$  spins/gram. With the exception of the increase in signal intensity, all signal parameters remained the same\*. Since the mechanical destruction of bone powder results in an increase in intensity of the resonance at  $g=2.008$  it is likely that the original powder resonance is due, at least in part, to the method of preparation of the samples, namely scraping with a glass slide. On this basis the reduced intensity of the whole bone resonance at  $g=2.008$  would reflect the reduced amount of preparation that is necessary to produce the sample. That is, if one assumes that the number of chemical bonds ruptured per gram is greater for the powder than for the whole bone samples and that the resonance amplitude is proportional to the number of ruptured bonds, then the results are intelligible. When samples of bone powder were heated to  $50^{\circ}\text{C}$  in air, they exhibited very large irreversible signal decreases indicating the presence of a chemically reactive free radical such as might be produced by mechanical damage.

It is likely that two different magnetic species are responsible for the resonances from bone, and that their relative

---

\* The production of a free radical by mechanical destruction and its subsequent stability is apparently a property of polymeric materials. For instance, germanium wafers subject to the same mechanical treatment shows no resonance at  $g=2.0$  at room temperature attributable to the mechanical treatment.

contribution to the resonance amplitude depends on whether the sample is examined as a powder, or whole. As a powder the damage induced free radical gives the dominant contribution: this accounts for the relatively high intensity of the powder resonance, and its increase when it is mechanically dispersed (Fig. 15). In whole bone samples the damage induced resonance may still be present, but a second species makes a significant contribution: this accounts for the relatively low intensity of the whole bone resonance and its difference in saturation behavior. It is also consistent with the differences seen when the temperature is lowered to 114°K.

The resonance at  $g=2.07$  has about the same  $g$ -value as has been found for the cupric ion absorbed on proteins (18). Since copper is known to be present in bone (19) in an amount greater than found here by EPR it is possible that the resonance is due to Cu(II). The difficulty is that the resonance is very weak, and is just resolved at 114°K in the most concentrated samples. A more definitive result could be probably obtained at lower temperatures where the hyperfine structure characteristic of the cupric ion might be resolved.

Some possible implications of the demonstrated property of bone to exhibit EPR absorption after mechanical damage are treated in the Conclusions. Presently, the nature of the magnetic species responsible for the absorption in both powdered and whole bone at  $g=2.008$  remains unknown. The whole bone resonance at  $g=2.008$  may

(17) Butyagin, P.: Doklady Akad. Nauk. S.S.S.R., 140, No. 1, 145, (1961).

(18) Walsh, W., Rupp, L. and Wyluda, B.: Paramagnetic Resonance, Vol. II, Low, W. (ed.), Academic Press, 1963, pg. 836.

(19) Becker, R., Spadaro, J. and Berg, E.: J. Bone & Joint Surg., (In Press).

represent a magnetic species that is naturally present in bone, in vivo. The results led us to search for a resonance in tendon collagen having properties comparable to those of whole bone and with an intensity of about  $1.0 \times 10^{16}$  spins/gram.  $[(4 \times 10^{16})/11.5 = 3.5 \times 10^{15}$  gives the number of spins per gram of whole bone, or per 0.35 gram of collagen if the resonance is assumed to arise from the protein moiety alone. Thus for collagen under this assumption we would expect  $3.5 \times 10^{15}/.35 \approx 1 \times 10^{16}$  spins/gram as an upper limit].

#### Collagen:

The EPR spectra of tendon collagen is a single line at  $g=2.007 \pm 0.003$  having a width between peaks of the derivative of  $10 \pm 1$  gauss. The line saturates homogeneously (12) with a weak maximum at about 10 db and shows no angular dependence. In addition to human tendon, the same resonance is found in bovine, rat, and dog tendon, suggesting that the responsible magnetic species may be associated with collagen per se and not just mammalian collagen. Accordingly, avian tendon (chicken) and amphibian tendon (frog) was examined and in both cases a single line with the same parameters was found. The intensity of absorption from human collagen corresponds to about  $4-14 \times 10^{15}$  spins/gram, which is about that expected on the basis of the results from whole bone. Magnetic field scans from 100 to 11,000 gauss at room temperature and at  $114^\circ\text{K}$  revealed no additional resonances in any human collagen samples. At  $114^\circ\text{K}$ , the resonance is saturated even at the lowest incident

microwave power level.

Samples of human tendon were examined by electron microscopy to determine whether the procedure of long term storage in a non-aqueous environment had produced protein denaturation thereby accounting for the singlet. The criterion used was the presence of the 640 A spacing which is a staining property of the native (undenatured) collagen fibril. The results showed that the 640 A spacing was indeed present and thus that protein denaturation had not occurred to any observable extent. In view of this, and of the minimal amount of handling necessary to prepare the samples, it was assumed that the EPR resonance was not an artifact and an effort was made to determine the nature of the magnetic species.

On the basis of the Rich-Crick model (20), collagen is not expected to exhibit paramagnetic absorption. A possibility of the origin of the line is a species of paramagnetic ion that is present in the protein either functionally or as a passive consequence of its presence in the interstitial fluid. Accordingly, the trace element content of tendon was examined by emission spectroscopy to determine if any paramagnetic ions of the iron group could be expected to be present in the amount indicated by EPR\*. The results of the trace element analysis are given in Figure 16. The spectrographic procedure is described in Appendix A. As can be seen virtually every element searched for is present in a sufficient amount to conceivably account for the observed resonance. A

---

\* The rare earth group is not considered since these elements are generally not found in biological material even in trace amounts ( $\sim 1$  ppm).

(20) Rich, A. and Crick, F.: J. Mol. Biol., 3, 483, (1961).

narrow isotropic resonance at  $g=2.0$  is not characteristic of iron group ions, but this possibility must nonetheless be considered. The situation is further complicated by the fact that since the observed resonance is so weak, it could be due to a paramagnetic ion not normally detected spectrographically in biological materials, a rare earth for instance. Thus, if the resonance is due to a paramagnetic ion, the number of possibilities is inordinately large. With reference to the iron group, it is probably safe to eliminate a few possibilities, the cupric ion for instance. The literature contains EPR studies of Cu(II) on or in various materials: spores (21), resins (22), proteins (23), and the nucleic acids (18). The (powder) spectrum of Cu(II) in these cases is characterized by the following: (a) the main absorption is found to have a  $g$ -value greater than  $g=2.04$ , (b) the width of the main absorption peak is greater than 40 gauss, (c) the presence of hyperfine structure is found. Since the resonance from collagen in no way resembles the powder spectrum normally found from Cu(II), it is reasonable to assume that Cu(II) is not the responsible species. Essentially the same argument can be made for manganese: the Mn(II) ion exhibits resolved hyperfine interaction resulting in a six line spectrum, rather than a single narrow line as seen from collagen. For titanium, Ti(III) usually yields resonances with  $g$ -values of 1.1 - 1.3 (24), much lower than that from collagen. Few of the remaining possibilities can be dismissed. It remains then to show

- 
- (21) Windle, J. and Sack, L.: *Biochim. Biophys. Acta*, 66, 173, (1963).  
(22) Farber, R. and Rodgers, M.: *J. Amer. Chem. Soc.*, 81, 1849, (1959).  
(23) Malmstrom, B. and Vanngard, T.: *J. Mol. Biol.*, 2, 118, (1960).  
(24) Bowers, K. and Owen, J.: *Repts. Progr. in Phys.*, 18, 304, (1955).

that an iron group ion could yield a sufficiently isotropic resonance at  $g=2.0$ . The best example is furnished by the cobalt ion. Dvir and Low (25) have found in a  $\text{CaF}_2$  crystal to which 0.1%  $\text{CoF}_2$  had been added, a sharp, slightly anisotropic line which they attributed to  $\text{Co(II)}$ . The resonance varied from  $g=2.010$  to  $g=2.0035$  and had a width of less than 15 gauss\*.

The unpaired electron species very often present in materials of biological origin is the "free radical" species. In particular, a free radical species has been reported by Forbes and Sullivan (7) in human tendon collagen. The EPR resonance, which is a 10 gauss singlet at  $g=2.0$  was produced by irradiation with 2537 Å light. No results were given for non-irradiated samples. When the constituent amino acids of collagen were individually irradiated, it was found that tyrosine gave a line most closely resembling that from irradiated collagen. On this basis, the EPR line from irradiated collagen was assigned to an unpaired electron located on the tyrosine residue. The results given here are for tendon collagen which has not been irradiated, except for normal room illumination. Even though the EPR results are similar to those from irradiated collagen, it was considered unlikely that the responsible magnetic species were identical in the two cases, particularly since the aromatic amino acids (e.g. tyrosine) are known to absorb strongly at 2537 Å and this wave length is negligibly present in room level illumination. This assumption

---

\* At 20°K hyperfine structure was barely resolved.

(25) Dvir, M. and Low, W.: Proc. Roy. Soc., (London), 75, 136, (1960).

was tested by examining commercial preparations of seventeen different amino acids found in human collagen\* (26). The amino acids were obtained as chromatographically pure crystalline powders and were exposed in quartz tubes to room illumination for a minimum of three weeks. None of the amino acids exhibited EPR absorption in the vicinity of  $g=2.0$  either before or after exposure to room illumination, indicating that the singlet from non-irradiated collagen is probably not due to a light-generated unpaired electron.

Since no EPR resonances are found in the constituent amino acids of collagen, it seems reasonable to conclude that the singlet from collagen is associated in some manner with the organization of the protein. The complexity of this organization and the very common EPR spectrum which is observed suggested that a fruitful approach would be to determine whether there exists any relationship between the EPR absorption and some of the known characteristics of collagen. Three of the most prominent characteristics of collagen are; (a) its three stranded helical structure, and the associated intramolecular bonds which stabilize the structure, (b) the 640 A banding it exhibits when stained with phosphotungstic acid and viewed under the electron microscope, (c) the phenomena of thermal shrinkage. All three are of course closely related. Thermal shrinkage, for instance, is believed to be a result of the weakening of intrachain hydrogen bonds (26) and results in the loss of 640 A banding (27). In this phenomenon, collagen fibers in

---

\* One additional amino acid which is present in human collagen, hydroxylysine, was not included because it was unavailable commercially.

(26) Gustavson, K.: The Chemistry and Reactivity of Collagen, Academic Press, 1956, pg. 39.

a fluid bath contract sharply and irreversibly to less than one-third their original length at a given temperature,  $T_g$ , the shrinkage temperature of collagen in that fluid. Normally, the fluid is water and for mammalian collagen  $T_g$  is 60-65°C (26). We have found no value in the literature for  $T_g$  in air or any gas. More recently than the comprehensive survey of the chemistry of collagen by Gustavson (26) the view was advanced that thermal shrinkage of collagen is a melting phenomenon akin to a crystalline → amorphous phase transition (28, 29). This view seems to have found acceptance by workers in the field (27, 30, 31).

The temperature dependence of the EPR signal from collagen in the interval about  $T_g$  is of interest because macroscopic shrinkage is indicative of some molecular process which may involve the unknown magnetic species. Since the experiment cannot be carried out in water, control experiments were performed to determine  $T_g$  in air. It was found that collagen can be heated to 100°C in air with no apparent change in the length of the fibers. This is not completely unexpected since it is known that  $T_g$  is roughly an inverse function of the dielectric constant of the fluid. Electron micrographs taken before and after heating show a narrower average fibril diameter after heating, but the 640 Å spacing is still present. At temperatures much above 100°C, the protein begins to decompose and as a result most experiments were confined below this temperature.

- 
- (27) Lowther, D.: International Review of Connective Tissue Research, Vol. I, Hall, D. (ed. ), Academic Press, 1963, pg. 79.  
(28) Garrett, R. and Flory, P.: Nature, 117, 176, (1956).  
(29) Flory, P. and Garrett, R.: J. Amer. Chem. Soc., 80, 4836, (1958).  
(30) Harrington, W. and Von Hippel, P.: Adv. in Prot. Chem., 1, (1961).

The temperature dependence of the EPR absorption of human tendon collagen was determined in the interval from 21°C to 95°C in atmospheres of air, pure nitrogen, and pure oxygen; the results are given in Figures 17a, c, e. They show the relative amplitude of the absorption signal as a function of temperature and are corrected for small changes ( $\sim 7\%$ ) in cavity Q which accompany heating. The corrections were made by referencing to a standard (single crystal of  $\text{CuSO}_4 \cdot 5\text{H}_2\text{O}$ ) which was in the same cavity as the collagen and was maintained at room temperature. Since the EPR absorption signal is relatively weak, the data in Figure 17 were taken by scanning through each point one hundred times and summing with a time averaging computer. This procedure gives an increase in the signal to noise ratio of ten. As can be seen there is a strong signal decrease in the vicinity of 70°C and the original signal intensity is not regained when the sample is cooled to room temperature. Also the results do not depend strongly on the nature of the gas environment. No change in line width or g-value is seen over the entire temperature range. In view of the apparent irreversibility of the signal decrease with temperature, the same samples were examined at room temperature at twenty-four hour intervals following the heating; a small daily increase was noted. At the end of two weeks the heating experiment was repeated and the results are given in Figures 17b, d, f. As can be seen, the original temperature dependence is exhibited. These results are

(31) Ramachandran, G.: International Review of Connective Tissue Research, Vol. I, Hall, D. (ed.), 1963, pg. 127.

for human tendon collagen, the entire experiment was repeated using dog tendon collagen and the results were identical. In none of the heating experiments did collagen exhibit fiber shrinkage.

In two weeks the strong temperature dependence is regained. One obvious physical process having a time constant of the order of days is the reacquisition by the protein of its normal water content which was driven off by heating. Accordingly, the role of water in the phenomenon was studied by vacuum drying samples of human tendon collagen (one week, base pressure  $10^{-6}$  Torr) and then heating. The resulting material displayed a temperature independent EPR absorption in the interval from 21°C to 95°C, suggesting that, in fact, water content is an important parameter. Two other methods of drying were employed; (a) long term storage over anhydrous  $\text{CaCl}_2$ , (b) immersion in dioxane\* for twenty-four hours. In both cases the dehydrated tendon collagen gave a temperature independent EPR absorption.

A well known degradation product of collagen is gelatin. It is produced by randomizing the helical structure of the parent molecule and is prepared commercially from animal skin. It was of interest to determine which, if any, of the results from tendon collagen are exhibited by gelatin. Gelatin prepared from pig skin was obtained in the form of flakes and reduced to powder either in a vibrating mill or by grinding with a mortar and pestle. This procedure produces free radicals in gelatin by rupturing chemical

---

\* A common dehydrating agent.

bonds and results in an EPR doublet with a splitting of 16 gauss (14). The doublet has been found here also, from gelatin derived from pig skin. Moreover, while the doublet decays as a doublet in vacuum, it is found to decay to a narrow singlet at  $g=2.008 \pm .003$  in the presence of air. The singlet has a width of  $11 \pm 1$  gauss and is stable indefinitely. The temperature dependence of the singlet both before and after vacuum drying is given in Figure 18. Figure 18b was obtained from gelatin which had been vacuum dried at a base pressure of  $10^{-6}$  Torr for one week. Vacuum drying was begun after the original doublet had decayed to a stable singlet. A strong temperature dependence analogous to that of collagen is seen, and the main effect of vacuum drying is to shift the region of strong signal decrease to a higher temperature range. Although it is not shown in Figure 18, the original room temperature amplitude is not regained upon cooling. Unlike the results from collagen, a signal increase with time and subsequent return of the temperature dependence is seen only inconsistently, and obviously involves factors not yet recognized.

The hydrothermal shrinkage phenomenon exhibited by collagen at  $70^{\circ}\text{C}$  suggested a comparison of the EPR intensity before and after shrinkage. Samples of human tendon collagen were immersed in water at  $70^{\circ}\text{C}$  for ten minutes, by which time they had obviously undergone thermal shrinkage. A comparison of the height of the absorption signal with that from the same sample before shrinkage

showed that the resonance had decreased in amplitude by an average of 50%; other signal parameters remained the same.

Returning to Figure 16, we see that there is about 10 ppm ( $\sim 10^{17}$  spins/gram) of copper in tendon collagen. Since +2 is a common valence state of copper and is paramagnetic, one might expect to see a copper EPR resonance. Since none is seen, it was conjectured that the large water loss exhibited by collagen as it equilibrates with room humidity after removal from the body might be responsible. In the absence of a sufficient amount of water, the Cu(II) might be so broadened as to be unobservable. According efforts were made to rehydrate the protein to the maximum amount permitted by EPR sensitivity considerations. This was accomplished by immersing samples of tendon collagen in pure water overnight and then allowing the thoroughly moistened samples to evaporate dry. A typical result is given in Figure 19a; a weak line at  $g=2.07$ , about 150 gauss wide. The superimposed narrow line is the normal (saturated) singlet at 2.008. While the presence of some magnetic species is indicated its identification as Cu(II) is not conclusive because of the lack of resolution. As a next step, Ringer's solution was substituted for pure water in an attempt to obtain a more resolved spectrum. Ringer's solution is a mixture of the chlorides of potassium, sodium and calcium and is routinely used to approximate the pH and ionic composition of interstitial fluid. By employing an ionic solution resembling the interstitial fluid,

it was intended that any possible leaching of Cu(II) into solution would be reduced, thereby enhancing the EPR line. The result, given in Figure 19b, is a well defined line showing resolved hyperfine structure which, as will be shown subsequently, is due to Cu(II).

Control experiments indicated that collagen has a great affinity for Cu(II) when it is added as a contaminant to Ringer's solution or pure water. Thus, there is the possibility that the spectrum in Figure 19b is the result of contamination, particularly since the spectrum, once it is produced, is stable. The question of whether the Cu(II) line is an artifact was not studied vigorously here, however, the affinity of the protein to absorb Cu(II) from weak solutions did suggest that useful information could be obtained by studying the EPR resonance parameters of the absorbed Cu(II).

There exists a number of theories attempting to explain the mechanism by which a collagen matrix can initiate mineralization, ossify, and turn to bone. Probably the most widely accepted are the theories of epitaxial growth in which it is assumed that certain regions along the fibril are sufficiently well ordered in the sense of forming a crystalline lattice that on the presence of certain enzymes crystal nucleation can take place\*. Given a crystal nucleus, the body fluids are sufficiently supersaturated to form a complete crystal spontaneously (32). A requisite in

---

\* The suggested mechanism is identical to that shown by many... inorganic salts. For instance, KI shows epitaxy on calcite, etc.

(32) Neuman, W. and Neuman, M.: Chemical Dynamics of Bone Mineral, Univ. of Chicago Press, 1956, pg. 170.

the theory is the existence of sites of well defined symmetry along the collagen fibers. Since EPR can be useful in determining the symmetry at a given site, and since Cu(II) is strongly absorbed it appeared that information concerning site symmetry in collagen could be obtained. Accordingly, samples of human tendon collagen were exposed to Cu(II) solutions in the range of 8-80  $\mu$ M (micromolar) for twenty-four hours at room temperature. The solid to solution ratio was 200 mg/1. The protein was rinsed and allowed to evaporate dry, and then examined by EPR. A typical result is given in Figure 19c. In the next section, the resonance will be shown to be a powder spectrum of Cu(II). For now we point out that the symmetry exhibited in Figure 19c does in fact support the concept of areas of crystalline order along the collagen fibers. The spectrum in Figure 19c, and hence the Cu(II) site, is characterized by a measurement of  $g_{11}$ ,  $g_1$ ,  $A'$ , and  $4B'$  made as indicated in Figure 19c. The results are  $g_{11} = 2.27$ ,  $g_1 = 2.07$ ,  $A' = 159$  gauss,  $4B' = 90$  gauss.

Apatite:

The EPR spectrum obtained from the cupric ion adsorbed on collagen serves to define a site of crystalline field symmetry on the protein. It was of interest to determine whether comparable sites exist on the mineral crystallites. The existence of such sites would support one concept of bone formation (epitaxial growth) and hence illuminate the nature of the apatite-collagen interface.

Accordingly, the absorption of the cupric ion onto bone mineral was studied in some detail.

The ground state of the free Cu(II) ion is  $3d^9 \ ^2D$ . In the solid state its five-fold orbital degeneracy is split in a manner determined by the symmetry of the crystalline electric field it experiences. In most copper containing ionic salts, the dominant symmetry is octahedral cubic with varying amounts of trigonal, tetragonal, and rhombic distortions mixed in (24). Under the action of an octahedral electric field the orbital levels split into an upper triplet and lower doublet. The doublet is further split into two orbital singlets under tetragonal or rhombic distortions. The Kramers (spin) degeneracy of the lower orbital singlet is removed by an external magnetic field giving rise to the observed EPR spectra of copper salts. Trigonal distortions do not split the lower doublet (33). In this case, the theorem of Jahn & Teller predicts that the copper complex will distort so as to remove the degeneracy and leave an orbital singlet lowest. There exists a series of such distortions and the system resonances through them resulting in a nearly isotropic g-value.

The EPR spectra of Cu(II) under cubic plus axial symmetry can be described by the following effective spin Hamiltonian:

$$H = g_{11} \beta H_z S_z + g_1 \beta (H_y S_y + H_x S_x) + A S_z I_z + B (S_x I_x + S_y I_y)$$

neglecting the nuclear Zeeman and quadrupole interactions.

(33) Bleaney, B., Bowers, K. and Trenam, R.: Proc. Roy. Soc., A, 228, 157, (1955).

$S$  = effective electron spin. (1/2)

$I$  = nuclear spin of copper ion. (3/2)

$g_{11}$  = g-value measured parallel to symmetry axis.

$g_1$  = g-value measured perpendicular to symmetry axis.

$\beta$  = Bohr magneton.

$(H_x, H_y, H_z)$  = components of external magnetic field.

$(A, B)$  = hyperfine coupling constants.

The corresponding energy levels to first order in the hyperfine coupling constants are (34):

$$E_+ = 1/2g\beta H + 1/2KM_I \quad [1]$$

$$E_- = - 1/2g\beta H - 1/2 KM_I \quad [2]$$

where

$$g^2 = g_{11}^2 \cos^2\theta + g_1^2 \sin^2\theta$$

$$K^2g^2 = A^2g_{11}^2 \cos^2\theta + B^2g_1^2 \sin^2\theta$$

and  $\theta$  is the angle between the electric field symmetry axis and the external magnetic field. The above two equations are sufficient to explain the resonances observed from Cu(II) adsorbed on bone mineral when provision is made for the fact that it is a powder spectrum.

The energy of a  $\Delta m = 1$  transition is

$$h\nu_0 = g\beta H + KM_I$$

defining

$$\frac{h\nu_0}{\beta} = H_0$$

we find that there is absorption of microwave energy for values of

$$H \text{ such that } H = \frac{H_0}{g} - \frac{KM_I}{g\beta} \quad [3]$$

(34) Bleaney, B.: Phil. Mag., [7], 42, 441, (1951).

Now, if  $dN$  is the number of spins having an electric field symmetry axis with the solid angle  $d\Omega$ , then, since one expects a random orientation of the symmetry axis:

$$\frac{dN}{d\Omega} = \frac{N_0}{4\pi}$$

or 
$$dN = \frac{N_0}{2} \sin\theta d\theta \quad [4]$$

where  $N_0$  is the total number of spins.

From [3] and [4] we may plot  $dN/dH$  versus  $H$  for each value of nuclear spin. As has been shown by Sands (35), the result for the case of  $I = 3/2$  is a set of four curves representing the theoretical distribution of line centers corresponding to the four possible nuclear orientations.

Samples of bone mineral were exposed intact (i.e. the same crystalline aggregate as in the original sample of refluxed bone) or as a powder to inorganic solutions containing known concentrations of  $\text{Cu(II)}$ . The ratio of the weight of the solid to volume of solution was held constant at about 500 mg/liter. Samples exposed as powders were recovered by centrifuging and rinsing several times in water, while those exposed as intact samples were simply rinsed, air dried, and then reduced to a powder. In all cases, the samples were exposed twenty-four hours at room temperature.

As has been discussed in Part I, bone mineral ("apatite") is generally regarded as an impure hydroxyapatite  $\text{Ca}_{10}(\text{PO}_4)_6(\text{OH})_2$ .

(35) Sands, R.: Phys. Rev., 99, 1222, (1955).

It was of interest to determine the naturally occurring trace elements of the iron group, particularly copper, found in bone mineral. No attempt was made to study calcium or phosphorus, or the per cent amorphous character of bone mineral. Results of a spectrographic analysis are given in Figure 20, the spectrographic procedure is described in Appendix A. The results show that the trace element content is negligible.

In addition to the trace element impurities, there are also present organic impurities due to the fact that refluxing with ethylenediamine is less than 100% efficient in removing the organic matrix. Electron micrographs of bone mineral prepared by refluxing with ethylenediamine show no traces of collagen (11): this agrees with a Kjeldahl analysis showing a nitrogen composition of 0.1% (11). Assuming that the organic residue is 16% nitrogen (about average for proteins) the analysis implies an organic fraction of about 0.6%.

The basic material not immersed in ionic solutions, was studied by EPR at magnetic fields of 100 to 11,000 gauss, at room temperature and at 114°K. No resonances were seen. When the samples were heated to 400°C for one hour, they exhibited a narrow resonance at  $g=2.0$  having a width of about 8 gauss. At first, it was thought that the line was a result of the creation of a point defect in the apatite by heating (36). Such defects have been reported in naturally occurring mineral apatites and are believed

(36) Becker, R. and Marino, A.: Nature, 210, 583, (1966).

responsible for their color (37). Subsequent work however, tends to indicate that the line is a result of charring of the organic residue. Lines corresponding to about  $10^{16}$  spins are easily formed by 500  $\mu\text{g}$  samples of collagen when heated to  $400^\circ\text{C}$  in air. This is about the amount of organic material present in each 100 mg apatite sample. Furthermore, while the signal created by heating is stable and does not change during either prolonged heating at  $400^\circ\text{C}$  or storage in air, it can be reduced by boiling the sample in water. Samples were first heated to  $400^\circ\text{C}$  for one hour and then boiled in water for one hour in an effort to dissolve the organic fraction. The resulting signal intensity was reduced by a factor of ten over that of non-boiled samples. Iterating the procedure does not further reduce the intensity. At  $600^\circ\text{C}$ , the line is completely wiped out.

When bone mineral was immersed in ionic solutions containing Cu(II), it exhibited a well defined Cu(II) EPR spectrum. A typical spectrum for Cu(II) adsorbed on apatite is given in Figure 21a. For solutions in the range 0.034 mM (millimolar) to 0.35 mM of Cu(II) the spectrum is sharp and distinct and the overall line shape remains constant. As the molarity is raised above 0.35 mM the low field lines are less resolved and the main absorption peak becomes featureless. These results do not depend on the nature of the anion. Equimolar solutions of the sulfate, nitrate, and chloride of Cu(II) yield identical spectra. Since we are interested in

(37) Vinokurv, V. and Zaripov, M.: Sov. Phys. Dokl., 6, 29, (1961).

detecting surface symmetry, the experiments were confined to solutions of 0.35 mM and below where the most amount of detail is present. Control experiments indicated that the shape of the curve did not depend strongly on whether the sample was immersed intact, or as a powder. Figure 21b shows the spectrum obtained from apatite immersed as a powder having a particle size of 150  $\mu$  or less. The principle difference between Figures 21a and b is the partial loss of resolution of the low field lines in Figure 21b. The intensity of absorption produced for a given molarity was much greater in the case of the powdered samples. The intensity of the EPR spectra of apatite immersed intact in a 0.035 mM solution is comparable to that of apatite immersed as a powder in 0.0035 mM. Figure 22 given the amount of Cu(II) absorbed onto intact samples of apatite as a function of the molarity. The concentrations of absorbed Cu(II) were found by emission spectroscopy. The results given in Figure 22 are of course dependent on the particular values of, solid to solution ratio, aggregate size, time, temperature, etc. that have been chosen. They do however, show a leveling off of which may be a "site saturation" effect. As the molarity is raised above 0.35 mM the amount of Cu(II) absorbed again begins to increase and becomes so large that it cannot be determined accurately by emission spectroscopy.

The spectrum in Figure 21 is a sum over the individual hyperfine lines of Cu(II) and over all values of  $\theta$ . It is typical for

Cu(II) in octahedral co-ordination with tetragonal distortion and has been found for Cu(II) in glass (35), spores (21), resins (22), proteins (23), and the nucleic acids (18). Equations [3] and [4] have been derived under just this assumed symmetry. From them we may graph  $dN/dH$  versus  $H$  for each of the four hyperfine lines. The results are given in Figure 23 together with the original derivative curve (Fig. 21a) and its intergral representation. The upper and lower field limits are:

$$H_U = \frac{H_0}{g_1} - \frac{BM_I}{g_1\beta}$$

$$H_L = \frac{H_0}{g_{11}} - \frac{AM_I}{g_{11}\beta}$$

The lower limits are a set of four equally spaced lines having a splitting of  $A/g_{11}\beta$  gauss centered at  $g_{11}$  while the upper set of four lines have a splitting of  $B/g_1\beta$  gauss centered at  $g_1$ . As can be seen in Figure 23, the sum of the derived curves closely approximate the actual absorption curve, even though we have assumed zero single crystal line width. The agreement may be made even better by assuming a finite line width for each of the individual hyperfine lines as has been shown by Vanngard and Aasa (38).

From Figure 23, we find the constants of the spin Hamiltonian are  $A = 0.017 \text{ cm}^{-1}$ ,  $B \leq 0.002 \text{ cm}^{-1}$ ,  $g_{11} = 2.27$ ,  $g_1 = 2.07$ .

The degree of resolution or sharpness of the EPR spectrum of Cu(II) adsorbed on apatite depends on the water content of the

(38) Vanngard, T. and Aasa, R.: Paramagnetic Resonance, Vol. II, Low, W. (ed.), Academic Press, 1963, pg. 509.

material indicating that at least some, possibly all, of the Cu(II) nearest neighbors are water molecules. The effect can be seen in Figure 24. The spectra were obtained by heating at the indicated temperature for twenty-four hours and then examining at room temperature. The loss of resolution from Figure 24a to Figure 24b is identical to that produced by vacuum drying at a base pressure of  $10^{-6}$  Torr. In order to detail the loss of resolution that accompanies heating, the previously identified char signal has been deleted from Figure 24.

To determine whether the electric field symmetry axis had any angular relation to the long axis of the bone from which the apatite was extracted, suitably prepared intact samples of apatite were studied. The resulting EPR spectrum was identical to that of Figure 21a for all angles between the magnetic field and the original long axis of the bone indicating that no such relationship exists. That is, the absorption per se produces a powder spectrum, because all crystal orientations are effectively present in a macroscopic sample.

#### Conclusions

The resonance from bone at  $g=2.008$  arises from: (a) a damage induced free radical created during the sample preparative procedure and (b) a naturally present free radical probably associated with the protein moiety.

The observed effect of the production of free radicals by

mechanical destruction may be of some importance in the process of fracture healing. Since a free radical is produced in bone by mechanical destruction in the laboratory it is reasonable to expect that an analogous situation will prevail at a fracture site in vivo. The initial response of the body to a fracture in the case of mammals is the proliferation of fibroblasts (collagen producing cells) and the mechanism by which these cells are "turned on" is presently unknown. Recently (39), in the case of amphibian fracture healing, the "trigger" has been shown to be an inhomogeneous electric field. It is suggested here that the distribution of free radicals that would be expected to be present over the surface of a fracture could provide sufficiently intense electric fields over cellular dimensions for this effect to function as the source of the trigger.

The singlet observed from tendon collagen is particularly interesting. Its existence was inferred by studying the bone singlet, and subsequently found to be present in all samples of mammalian collagen studied. Spectrographic analysis does not preclude the possibility that the line is due to a paramagnetic ion. However, none of the constituent amino acids exhibit EPR absorption when examined individually so that this possibility may reasonably be eliminated. The magnetic species may be a free radical which is a result of the organization of the protein. Since what appears to be the same resonance is seen in gelatin, the species

---

(39) Becker, R. and Murray, D.: Trans. of the N.Y. Acad. of Sci., 29, 606, (1967).

is probably associated with an individual polypeptide chain rather than the entire molecule.

The temperature dependence of the collagen singlet in air, nitrogen and oxygen exhibits a strong decrease at 60°-70°C, which is just the temperature interval in which the phenomenon of hydrothermal shrinkage occurs. The two may be related. Since thermal shrinkage is itself poorly understood little insight into the nature of the phenomenon reported here is gained. Nevertheless, the decrease of the EPR resonance may reflect some change on the molecular level which precedes and results in the macroscopic effect of shrinkage. The importance of water in the temperature dependence of the singlet is indicated. Water may act as an activator lowering the amount of energy necessary for some process to "go". An identical role for water has been found in the process of electrical conduction of proteins (40). Such an assumption fits the results for gelatin (Fig. 18), where the effect of vacuum drying is to shift the region of maximum decrease to higher temperatures. Also, the results for vacuum dried collagen may be interpreted as showing that the strongly temperature dependent region is shifted to temperatures greater than 100°C.

Further work is needed to definitely identify the responsible magnetic species, and the mechanism involved in the strong temperature decrease.

Copper has been found spectroscopically in human tendon, however

---

(40) Rosenberg, B.: J. Chem. Phys., 36, 816, (1962).

the identification of naturally occurring Cu(II) by EPR is, presently, not conclusive. Tendon collagen, doped with Cu(II) exhibited a well defined Cu(II) EPR spectrum characterized by:  $g_{11} = 2.27$ ,  $g_1 = 2.07$ ,  $A' = 159$  gauss ( $A = .017 \text{ cm}^{-1}$ ),  $4B \leq 90$  gauss ( $B \leq .002 \text{ cm}^{-1}$ ). This indicates that there exist sites along the collagen fiber at which the concept of crystalline order is valid.

Bone mineral extracted by refluxing with ethylenediamine exhibits no resonances in agreement with the results of a spectroscopic study. The narrow singlet that develops when apatite is heated is in all probability the result of charring of the residual organic fraction ( $\sim 0.6\%$ ). This is borne out by the observation that amounts of organic material known to be present can produce such a resonance and of comparable intensity when heated. Furthermore, since the organic material will have a finite solubility in boiling water one would expect the resonance created by heating to be reduced by boiling, and this is observed.

Apatite exposed to solutions containing Cu(II) readily takes up the metallic ion from solution. There is short range order about the Cu(II) sites in apatite as evidenced by the symmetry of the EPR absorption spectrum. When the molarity of the solution is below 0.35 mM of Cu(II), the spectrum can be described by an axially symmetric Hamiltonian having constants  $g_{11} = 2.27$ ,  $g_1 = 2.07$ ,  $A = 0.017 \text{ cm}^{-1}$ ,  $B \leq 0.002 \text{ cm}^{-1}$ . The constants are consistent with the assumption of octahedral co-ordination for Cu(II) with a

tetragonal distortion. Comparable although not identical values have been found in all of the previously mentioned studies of Cu(II) absorption (18, 21, 22, 23, 35).

Almost certainly some and possibly all of the Cu(II) nearest neighbors are water molecules. The evidence for this is the decrease in signal intensity and resolution when heating is begun. As the apatite is dehydrated the degree of symmetry of the electric field at the Cu(II) sites diminishes, resulting in a less resolved spectrum. Significantly, the symmetry of the Cu(II) sites is not completely destroyed until temperatures of 600°C are reached. At 110°C there is a partial loss of resolution. At this temperature all of what is termed the "surface adsorbed" or "non-essential" water is driven off from both of the major prototypes of bone mineral HA (32) and OCP (41). It is reasonable to assume that the same situation will prevail for bone mineral, or equivalently that the partial loss of resolution between room and 110°C is due to surface desorption. The electric field symmetry present at the Cu(II) sites as manifest in Figure 24b through Figure 24f is a result of the presence of more strongly bound water. That is, the Cu(II) nearest neighbors are water molecules, some on the surface and some more strongly bound, possibly occupying lattice positions in the crystallites. As has been pointed out in Part I lattice water is presumed to be present in HA, while OCP is known to contain water of crystallization. The complete loss of the Cu(II)

---

(41) Brown, W.: Nature, 196, 1048, (1962).

line between 500° and 600°C is in particularly good agreement with the results for HA where it is found that at these temperatures the material is completely dehydrated.

The cupric ion absorbed onto tendon collagen and bone apatite yields a similar EPR spectrum in each case. The set of four constants of the spin Hamiltonian which characterizes each resonance are, within experimental error, identical for the two materials. Since the symmetry of the EPR spectrum directly reflects the symmetry of the paramagnetic ion site, the results indicate that there exists sites of the same symmetry on each material. To give some idea of the spread in the spin Hamiltonian constants describing the powder spectrum of absorbed Cu(II), some representative values from the literature are given in Figure 25. The virtual identity of the constants for apatite and collagen as compared with the spread in values shown in Figure 25 is what is meant by "sites of the same symmetry" on collagen and apatite.

A number of structural relationships between the organic and inorganic components of bone are known, based on studies by X-ray diffraction and electron microscopy. The interrelationships have led to a concept of bone growth invoking the mechanism of epitaxial growth (32). That is, the orientated overgrowth of bone mineral on certain well-crystallized areas of the organic matrix. The proposed mechanism differs in principle from that of older theories of bone growth which we refer to collectively as the precipitation

theories. Such theories assign no active role to the organic matrix in the mineralization process and account for ossification by assuming that the interstitial fluid becomes temporarily super-saturated in certain regions resulting in spontaneous crystal precipitation. Epitaxial growth, on the other hand, ascribes an active role to the organic matrix; that of the seed-forming agent. One requirement for the seeding of apatite is that the lattice spacings on the surface of apatite and the substrate must be almost identical, or in simple numerical ratio. The results found here support the concept of epitaxial growth to the extent that they show that there are areas of identical crystal order on apatite and the organic substrate as would be required in epitaxial growth. Hence the copper-binding sites in apatite and tendon may be sites which under proper conditions in vivo are linked to form bone.

The collagen that has been studied here is tendon collagen; a structure which normally does not calcify. For this reason, it has long been recognized that mineralization is a more complicated process than just an interaction between the protein collagen and inorganic ions in the interstitial fluid. There have been a number of attempts to find a "local factor" in the process of mineralization; that is, a factor present in normally calcifiable collagen which could in some manner account for crystal nucleation. All such attempts have thus far been unsuccessful. Thus, the initiation of mineralization obviously involves more than areas of fixed

symmetry as have been detected by EPR. The hypothesis here is that when mineralization is initiated it occurs at the sites which in these experiments are occupied by copper.

Where are the copper-binding sites in tendon? Since tendon is 95% collagen it seems obvious to suspect that they are located directly on the protein per se. This may of course not be the case. The question could possibly be answered by examining the EPR spectrum of Cu(II) adsorbed onto tendon which has been subjected to various degrees of "purification". It is possible to remove certain components of the ground substance of tendon by chemical methods. By a systematic chemical treatment followed by a Cu(II) absorption study, the location of the copper-binding sites might be determined.

The results given here suggest that water and/or copper may have an important role in the mineralization process; a role heretofore unrecognized.

As an alternative to the direct overgrowth of apatite on collagen, consider the following. There is one substance which is universally present at the collagen-apatite interface; water. The presence of ordered water molecules in tendon collagen as detected by Nuclear Magnetic Resonance has been reported by Berendsen (42). He found that his results could best be described by assuming that the water molecules formed chains in the direction of the collagen fiber axis which were hydrogen bound to the protein. The water contained on apatite also exhibits some form of structure,

---

(42) Berendsen, H.: J. Chem. Phys., 36, 3297, (1962).

at least that part which is co-ordinated to the Cu(II) sites. It is suggested that collagen and apatite may not be linked directly, but through mutual bonding to an interfacial layer of water. The water layer which may vary from one to several layers in thickness is hydrogen bonded to the protein, and occupies a lattice position in the mineral (HA) or is present as water of crystallization (OCP).

In the case of copper, there is an increasing amount of circumstantial evidence indicating that it may be of importance in the mineralization process.

(a). Copper has been proposed as a possible activator in the fluorescence of bone (43). That is, copper appears to be associated with the fluorescence mechanism of the apatite-collagen complex. Thus, it may be important in collagen function.

(b). Copper content of bone is relatively constant over a large temporal range (19). It was found by spectroscopic comparison of modern and ancient (~ 500 years old) bone that the copper content was remarkably constant at 1 to 5 ppm of bone ash. This may mean that copper is of functional importance in the bone matrix.

(c). While the detection of naturally occurring cupric ions in bone and tendon collagen is tentative, it is established here that the ion resides in sites of identical crystal field symmetry when adsorbed onto apatite and tendon collagen. It is possible that in bone the cupric ion is shared by collagen and apatite and in this manner links the two materials.

---

(43) Bachman, C. and Ellis, E.: Nature, 206, 1328, (1965).

Much of the preceeding is speculation and a considerable refinement is necessary. However, the ideas that (a) water may be quite literally the cementing substance in bone and (b) that copper may play an important role in bone formation, are worthy of further work.

## Appendix A - Spectrographic Procedure\*

1. Instrument

1.5 meter Wadworth Spectrograph (Jarrell-Ash);  
2000 + 4000 A region, grating - second order, 590 lines/mm.  
microphotometer-comparator (Jarrell-Ash).

2. Output

35 mm film, SA-1.

3. Method

D.C. arc in air, anode excitation.

4. Parameters

electrodes: graphite (SPK), lower cupped, upper rounded.

gap: 8 mm

slit: 10  $\mu$

time: 60 sec.

load: 10 mg

current: 10 amps (nominal)

5. Standards

Prepared by addition of known amounts of powdered  $\text{CuSO}_4$  to spectroscopically pure  $\text{CaCO}_3$  (for copper concentration analysis).

S.Q. powders for trace element analyses.

6. Procedure

All standards and unknowns mixed 1/9 with buffer composed of equal parts of spectrographically pure  $\text{LiCO}_3$  and SP-2 graphite.

---

\* Performed by Mr. Joseph Spadaro whose Dissertation, (currently in progress), contains a more complete description of the procedure and results.

## Bibliography

## Part I

- (1) Bloom, W. and Fawcett, D.: Histology, Saunders Co., 1964.
  - (2) Glimcher, M.: Rev. Mod. Phy., 31, 361, (1959).
  - (3) Frost, H.: Bone Remodelling Dynamics, Thomas Co., 1963.
  - (4) Robinson, R.: J. Bone & Joint Surg., 34-A, 389, (1952).
  - (5) Ramachandran, G.: International Review of Connective Tissue Research, Vol. I, Hall, D. (ed.), Academic Press, 1963, pg. 138.
  - (6) Cochran, W., Crick, R., and Vand, V.: Acta Cryst., 5, 581, (1952).
  - (7) Rich, A. and Crick, F.: J. Mol. Biol., 3, 483, (1961).
  - (8) Bear, J.: Biophys. Biochem. Cytol., 2, 363, (1956).
  - (9) Ramachandran, G. and Kartha, G.: Nature, 176, 593, (1955).
  - (10) Gustavson, K.: The Chemistry and Reactivity of Collagen, Academic Press, 1956.
  - (11) Posner, A.: Clin. Orthoped., 9, 5, (1957).
  - (12) Ellis, E.: Ph.D. Dissertation, Syracuse University, (1964).
  - (13) DeJong, W.: Rec. Trav. Chem., 45, 445, (1926).
  - (14) Naray-Szabo, St.: Ztschr. Krist., 75, 387, (1930).
  - (15) Carlstrom, D.: Acta Radiol., Supp. 121, (1955).
  - (16) Engstrom, A. and Finean, J.: Nature, 171, 564, (1953).
  - (17) Finean, J. and Engstrom, A.: Biochim. Biophys. Acta, 11, 128, (1953).
  - (18) Robinson, R. and Watson, M.: Anat. Rec., 114, 383, (1952).
  - (19) Neuman, W. and Neuman, M.: Chemical Dynamics of Bone Mineral, Univ. of Chicago Press, 1958.
-

- (20) Posner, A. and Perloff, A.: J. Res. Nat. Bureau, Stand., 58, 279, (1957).
- (21) Hendricks, S. and Hill, W.: Proc. Nat. Acad. Sci., 36, 731, (1950).
- (22) Brown, W., Lehr, J., Smith, J., and Frazier, A.: J. Am. Chem. Soc., 79, 5318, (1957).
- (23) Arnold, P.: Trans. Faraday Soc., 46, 1061, (1950).
- (24) Brown, W., Lehr, J., Smith, J., and Frazier, A.: Nature, 196, 1050, (1962).
- (25) Brasseur, H., Dallemagne, M., and Melon, J.: Nature, 157, 453, (1946).
- (26) Harper, R. and Posner, A.: Proc. Soc. Exp. Bio. Med., 122, 937, (1966).
- (27) Termine, J. and Posner, A.: Science, 153, 1523, (1966).

#### Part II

- (1) Berendsen, H.: J. Chem. Phys., 36, 3297, (1962).
  - (2) Yevdokimova, Y. and Varshavskii, Y.: Biofizika, 11, No. 1, 7, (1966).
  - (3) Rosenberg, B.: J. Chem. Phys., 36, 816, (1962).
  - (4) Ling, G.: Fed. Proc., Fed. Am. Soc. Ex. Bio., 25, No. 3, Part 1, 958, (1966).
  - (5) LaBella, F. and Paul, G.: J. Gerontol., 20, 54, (1965).
  - (6) Bull, H.: J. Amer. Chem. Soc., 66, 1499, (1944).
  - (7) Rosen, D.: Trans. Faraday Soc., 59, 2178, (1963).
  - (8) Frost, H.: Bone Remodelling Dynamics, Thomas Co., 1963.
  - (9) Bassett, C. and Becker, R.: Science, 137, 1063, (1962).
  - (10) Becker, R., Bassett, C., and Bachman, C.: Bone Biodynamics, Frost, H. (ed.), Little, Brown, & Co., 1964.
-

- (11) Balwin, M. and Morrow, J.: J. Chem. Phys., 36, 1591, (1962).
- (12) Kurosaki, S.: J. Phys. Chem., 58, 320, (1954).
- (13) Nelson, S., Newman, A., Tomlinson, T., and Sutton, L.: Trans. Faraday Soc., 55, 2186, (1959).
- (14) Brunauer, S., Emmett, P., and Teller, E.: J. Amer. Chem. Soc., 60, 309, (1938).
- (15) Lange, N.: Handbook of Chemistry, 1949, pg. 1432.
- (16) Neuman, W., Toribara, T., and Mulryan, B.: J. Amer. Chem. Soc., 75, 4239, (1953).
- (17) Marton, L.: Methods of Experimental Physics, 6, Part B, Academic Press, 1959, pg. 9.
- (18) Debye, P.: Polar Molecules, Dover Publications, 1929.
- (19) Boyd, W.: Textbook of Pathology, Lea & Febiger, 1961.
- (20) Bather, R., Webb, S., and Cunningham, T.: Nature, 207, 30, (1965).

### Part III

- (1) Slager, V. and Zucker, M.: Transplant. Bull., 30, 146, (1962).
  - (2) Cole, T. and Silver, A.: Nature, 200, 700, (1963).
  - (3) Swartz, H.: Radiation Res., 24, 579, (1965).
  - (4) Termine, J., Pullman, I., and Posner, A.: Arch. Biochem. Biophys., 122, 318, (1967).
  - (5) Becker, R.: Nature, 199, 1304, (1963).
  - (6) Commoner, B.: In Proc. Conf. Aseptic Necrosis of the Femoral Head, St. Louis, Mo., 1964.
  - (7) Forbes, W. and Sullivan, P.: Biochim. Biophys. Acta, 120, 222, (1966).
  - (8) Patten, R. and Gordy, N.: Rad. Res., 22, 29, (1964).
-

- (9) Becker, R., Bassett, C., and Bachman, C.: Bone Biodynamics, Frost, H. (ed.), Little, Brown, & Co., 1964.
  - (10) Becker, R. and Brown, F.: *Nature*, 200, 700, (1965).
  - (11) Williams, J. and Irvine, J.: *Science*, 119, 771, (1954).
  - (12) Portis, A.: *Phys. Rev.*, 91, 1071, (1953).
  - (13) Ulbert, L.: *Nature*, 195, 175, (1962).
  - (14) Abagyan, G. and Butyagin, P.: *Biofizika*, 9, No. 2, 180, (1964).
  - (15) Bresler, S., Zhurkov, S., Kasbekov, E., Saminskii, E. and Tomashevskii, E.: *J. Tech. Phys. U.S.S.R.*, 29, 358, (1959).
  - (16) Ulbert, K. and Butyagin, P.: *Doklady Akad. Nauk. S.S.S.R.*, 149, No. 5, 1194, (1963).
  - (17) Butyagin, P.: *Doklady Akad. Nauk. S.S.S.R.*, 140, No. 1, 145, (1961).
  - (18) Walsh, W., Rupp, L., and Wyluda, B.: Paramagnetic Resonance, Vol. II, Low, W. (ed.), Academic Press, 1963, pg. 836.
  - (19) Becker, R., Spadaro, J., and Berg, E.: *J. Bone & Joint Surg.*, (In Press).
  - (20) Rich, A. and Crick, F.: *J. Mol. Biol.*, 3, 483, (1961).
  - (21) Windle, J. and Sack, L.: *Biochim. Biophys. Acta*, 66, 173, (1963).
  - (22) Farber, R. and Rodgers, M.: *J. Amer. Chem. Soc.*, 81, 1849, (1959).
  - (23) Malmstrom, B. and Vanngard, T.: *J. Mol. Biol.*, 2, 118, (1960).
  - (24) Bowers, K. and Owen, J.: *Repts. Progr. in Phys.*, 18, 304, (1955).
  - (25) Dvir, M. and Low, W.: *Proc. Roy. Soc., (London)*, 75, 136, (1960).
  - (26) Gustavson, K.: The Chemistry and Reactivity of Collagen, Academic Press, 1956, pg. 39.
-

- (27) Lowther, D.: International Review of Connective Tissue Research, Vol. I, Hall, D. (ed.), Academic Press, 1963, pg. 79.
- (28) Garrett, R. and Flory, P.: Nature, 117, 176, (1956).
- (29) Flory, P. and Garrett, R.: J. Amer. Chem. Soc., 80, 4836, (1958).
- (30) Harrington, W. and Von Hippel, P.: Adv. in Prot. Chem., 1, (1961).
- (31) Ramachandran, G.: International Review of Connective Tissue Research, Vol. I, Hall, D. (ed.), 1963, pg. 127.
- (32) Neuman, W. and Neuman, M.: Chemical Dynamics of Bone Mineral, Univ. of Chicago Press, 1956, pg. 170.
- (33) Bleaney, B., Bowers, K. and Trenam, R.: Proc. Roy. Soc., A, 228, 157, (1955).
- (34) Bleaney, B.: Phil. Mag., [7], 42, 441, (1951).
- (35) Sands, R.: Phys. Rev., 99, 1222, (1955).
- (36) Becker, R. and Marino, A.: Nature, 210, 583, (1966).
- (37) Vinokurv, V. and Zaripov, M.: Sov. Phys. Dokl., 6, 29, (1961).
- (38) Vanngard, T. and Aasa, R.: Paramagnetic Resonance, Vol, II, Low, W. (ed.), Academic Press, 1963, pg. 509.
- (39) Becker, R. and Murray, D.: Trans. of the N.Y. Acad. of Sci., 29, 606, (1967).
- (40) Rosenberg, B.: J. Chem. Phys., 36, 816, (1962).
- (41) Brown, W.: Nature, 196, 1048, (1962).
- (42) Berendsen, H.: J. Chem. Phys., 36, 3297, (1962).
- (43) Bachman, C. and Ellis, E.: Nature, 206, 1328, (1965).

### Acknowledgements

I am indebted to Dr. Charles H. Bachman for his advice and assistance throughout the course of this work, and also for his enthusiasm for the area of Biophysics which I have come to appreciate.

I wish to thank Mr. Frederick Brown and Mr. Daniel Harrington for many helpful and informative discussions concerning the biological sciences, and Mr. Joseph Spadaro for his advice and help readily given a great many times during the course of these experiments. I am particularly grateful to Mr. Spadaro for performing the spectrographic analyses.

I wish to express thanks to Mrs. Donna Hammill for her cooperation and competence in typing the entire manuscript, and Mr. Allen Ayers for his art work in preparing the illustrations.

For his ideas which permeate these pages, and for his constant advice and guidance, I gratefully acknowledge a debt I can never repay to Robert O. Becker, M.D., Doctor.

I wish to extend my greatest thanks to my wife, Linda, for her constant support and encouragement which was an invaluable aid to me during the course of these investigations.

## Vita

Name	Andrew Anthony Marino
Date and Place of Birth	January 12, 1941, Philadelphia, Pennsylvania
Elementary School	Most Blessed Sacrament, Philadelphia, Pennsylvania
Graduated	June 1954
High School	West Philadelphia Catholic, Philadelphia, Pennsylvania
Graduated	June 1958
College	St. Joseph's College, Philadelphia, Pennsylvania
Degree	B.S. - Physics
Date	June 1962
Graduate School	Syracuse University, Syracuse, New York
Appointments	Teaching Assistant, September 1963 - June 1964
Degrees and Dates	M.S. - Physics, June 1965 Ph.D. - Physics, June 1968

---

## Table of Illustrations

Figure Number	Title
1.	Longitudinal Section of Cortical Bone
2.	Cross Section of Cortical Bone
3.	Structural Organization of Mammalian Collagen
4.	The Rich-Crick Models of Collagen
5.	The Crystal Structure of Hydroxyapatite
6.	Humidities Maintained By Saturated Solutions
7.	Direct Current Conductivity of Bone
8.	Dielectric Constant of Bone as a Function of Frequency
9.	Dielectric Constant of Bone as a Function of Hydration
10.	Dielectric Loss of Bone as a Function of Frequency
11.	Dielectric Loss of Bone as a Function of Hydration
12.	The Critical Hydration of Bone
13.	Average Adsorption Isotherm of Bone
14.	Dielectric Constant of Pathological Bone
15.	Accumulation of Free Radicals in Bone
16.	Iron Group Trace Elements in Human Tendon Collagen
17.	Temperature Dependence of EPR Signal from Tendon
18.	Temperature Dependence of EPR Signal from Gelatin

---

19. EPR Spectrum from Tendon Collagen Under Various Conditions
  20. Iron Group Trace Elements in Bone Mineral
  21. EPR Spectrum of Cupric Ion Absorbed on Bone Mineral
  22. Uptake of Cupric Ion by Bone Mineral
  23. Theoretical Distribution of Line Centers for Adsorbed Cupric Ions
  24. Change in EPR Spectrum of Cupric Ion Absorbed on Bone Mineral Produced by Heating
  25. Representative Values from the Literature for Spin Constants
-

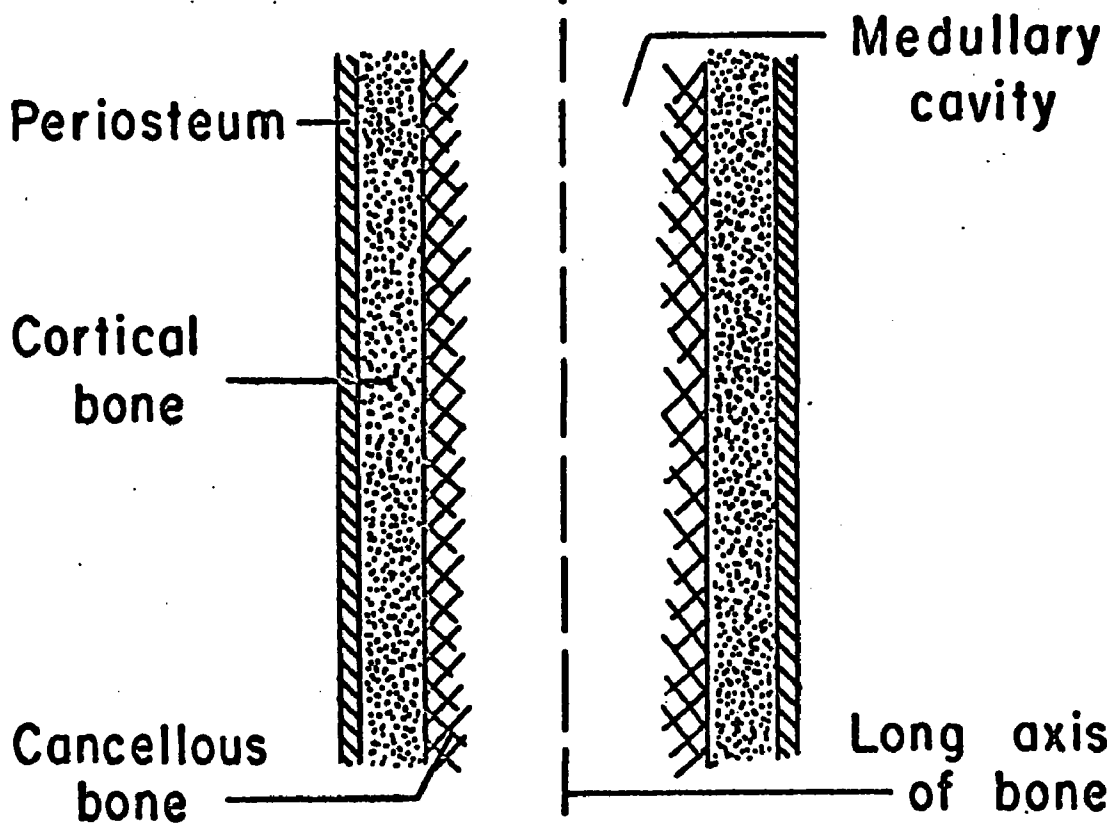


Figure 1. Longitudinal section of the midshaft region of a typical long bone.

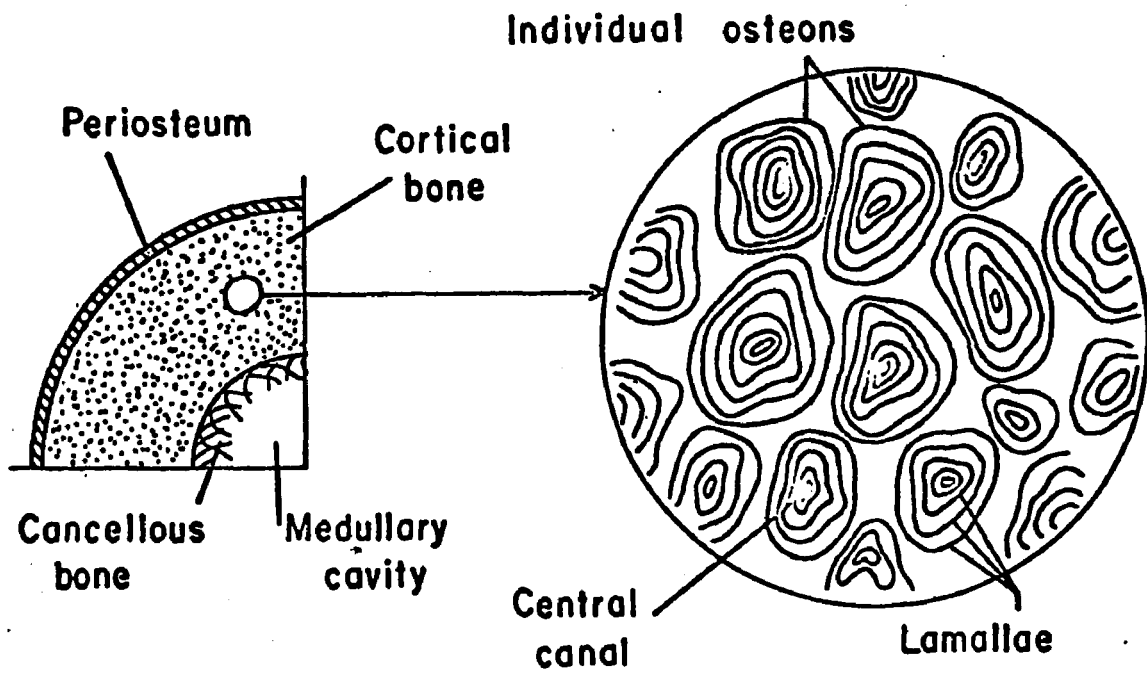


Figure 2. Sector of a cross section of a typical long bone. The location of the individual osteons is depicted.

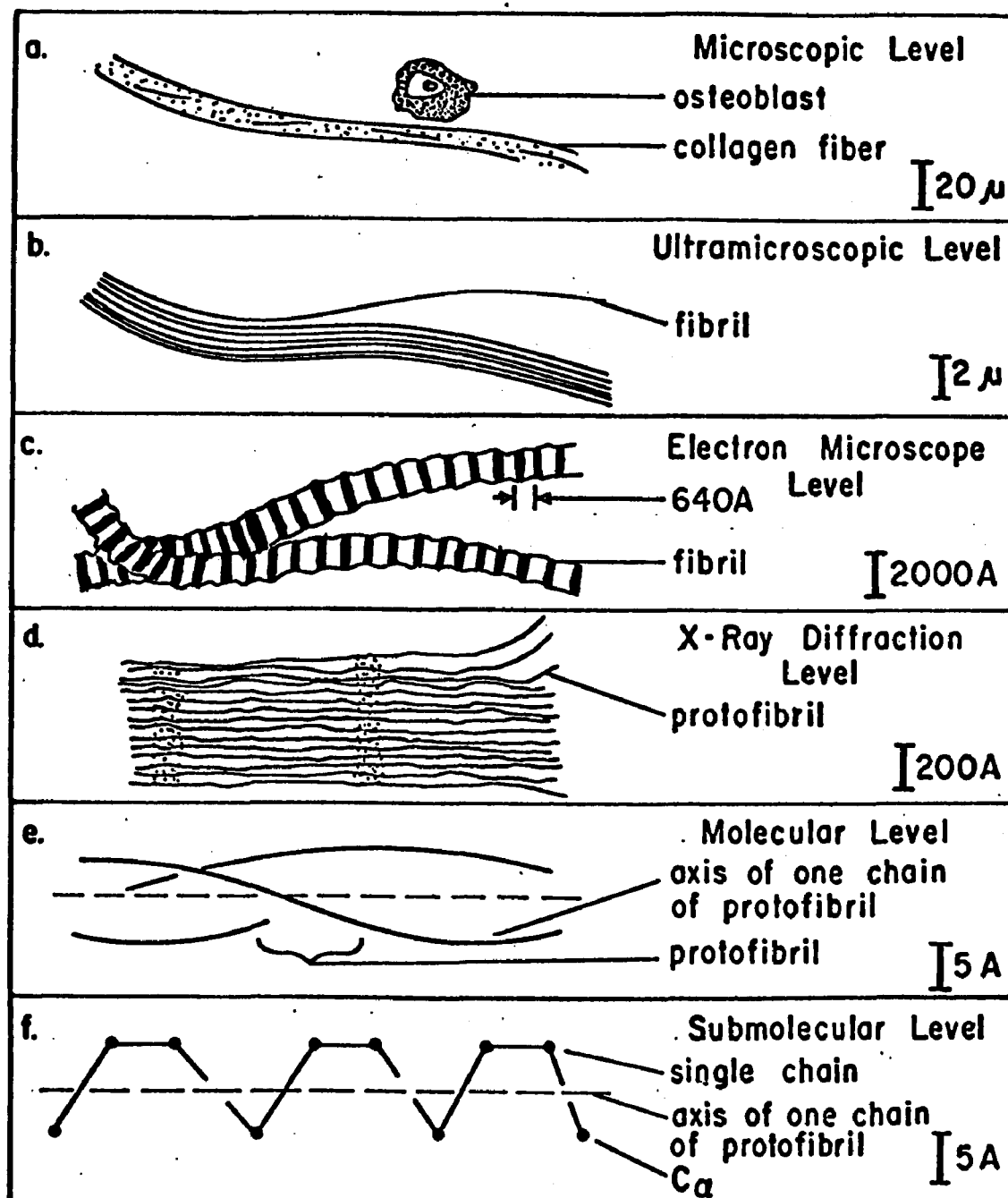


Figure 3. Structural organization of mammalian collagen.

Adapted from Bear, R.: Adv. Prot. Chem., 7, 72, (1952), Fig. 1.

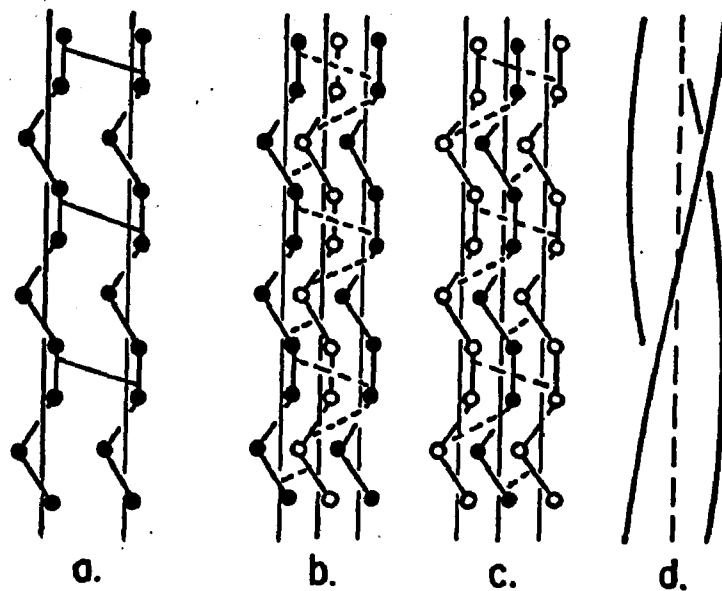


Figure 4. The Rich-Crick models of collagen, adapted from reference (7), Part I. Only the  $C_{\alpha}$  atoms are shown. Chains composed of atoms depicted by circles lie in front of those depicted by dots.

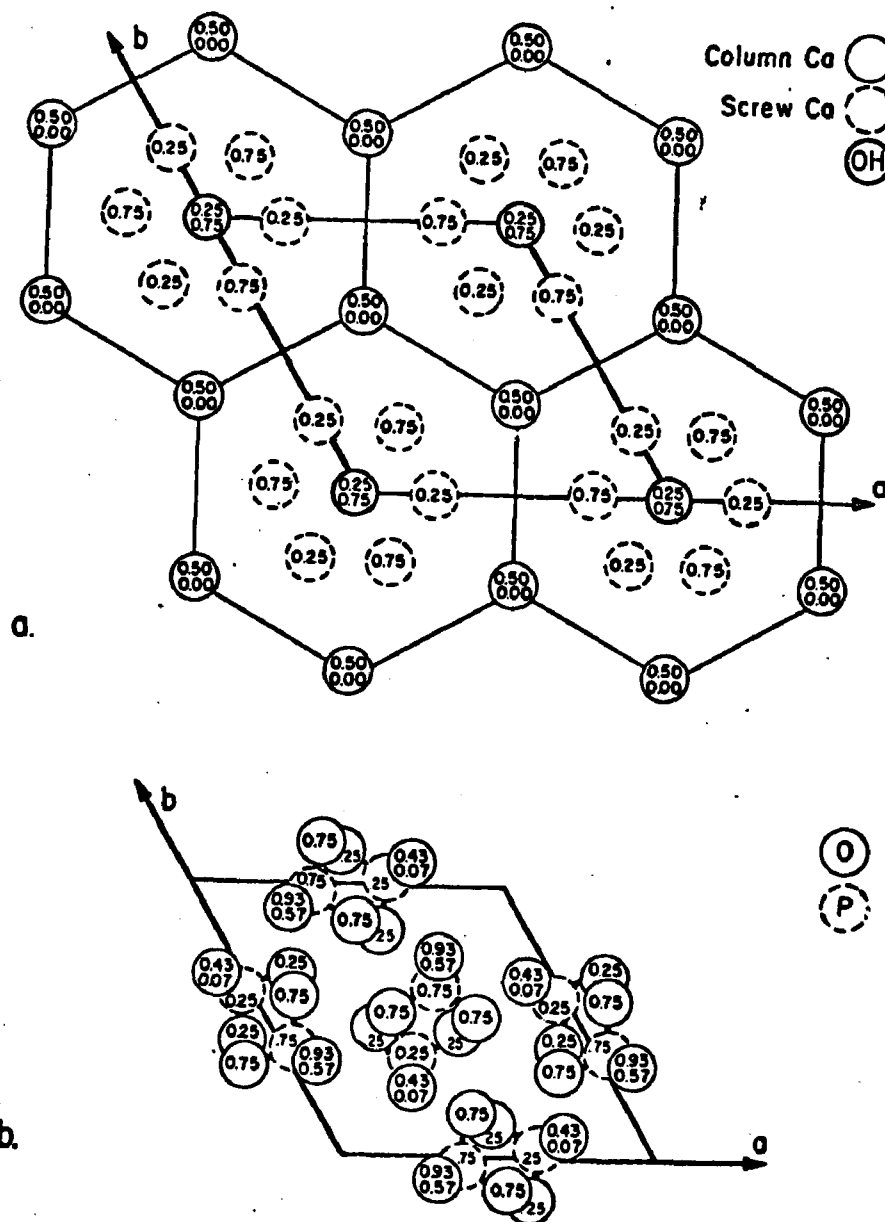


Figure 5. Hydroxyapatite structure: projected down the c-axis onto the 001 plane. Adapted from Kay, M., Young, R., Posner, A.: *Nature*, 204, 1050, (1964). The numbers represent the fractional height in the c-axis direction. The unit cell dimensions are:  $a = b = 9.43 \text{ \AA}$ ,  $c = 6.88 \text{ \AA}$ .

(a) The positions of the calcium and the hydroxyl ions. More than the unit cell is illustrated. The "columnar" calcium ions are located at the corners of hexagons. The "hexagonal screw" calcium ions form channels in which the hydroxyl ions (corners of the unit cell) are situated.

(b) The location of the phosphate groups.

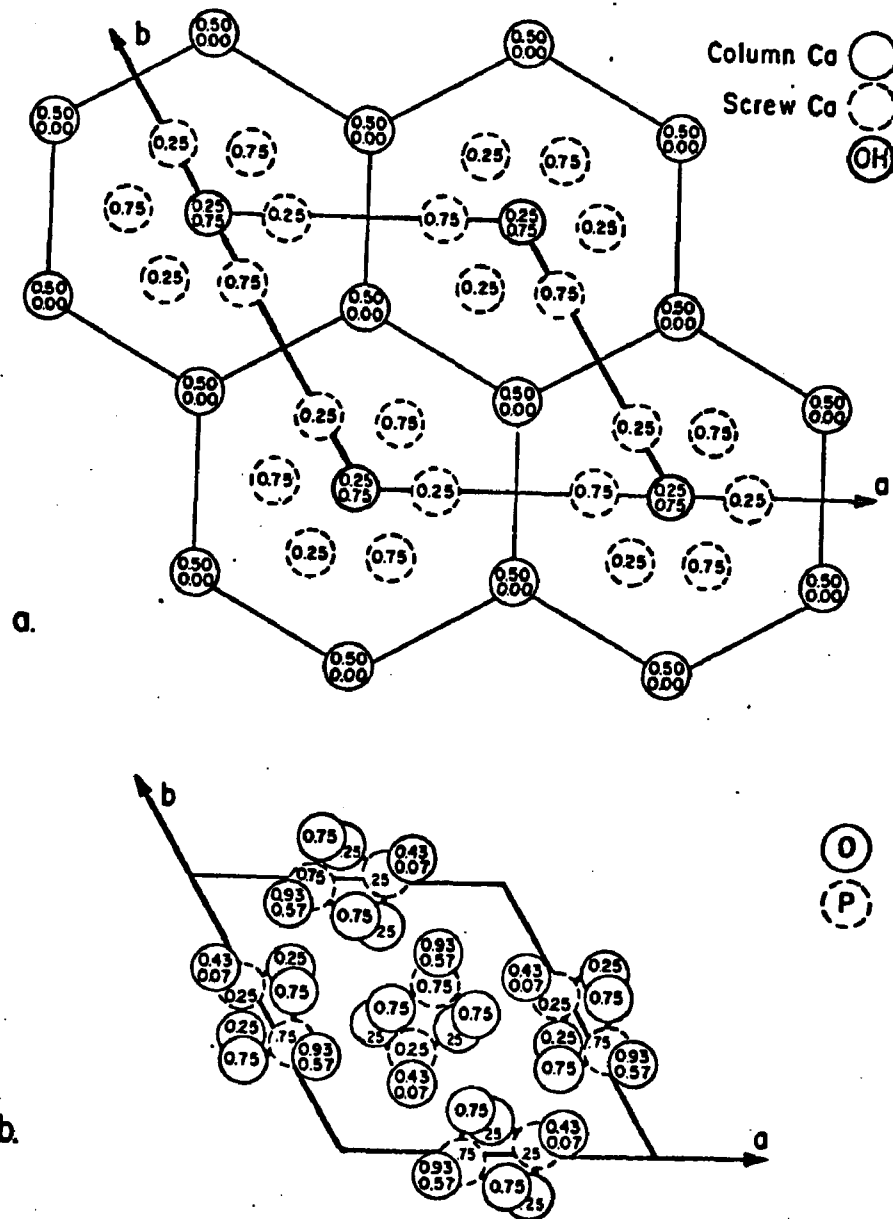


Figure 5. Hydroxyapatite structure: projected down the c-axis onto the 001 plane. Adapted from Kay, M., Young, R., Posner, A.: *Nature*, 204, 1050, (1964). The numbers represent the fractional height in the c-axis direction. The unit cell dimensions are:  $a = b = 9.43 \text{ \AA}$ ,  $c = 6.88 \text{ \AA}$ .

(a) The positions of the calcium and the hydroxyl ions. More than the unit cell is illustrated. The "columnar" calcium ions are located at the corners of hexagons. The "hexagonal screw" calcium ions form channels in which the hydroxyl ions (corners of the unit cell) are situated.

(b) The location of the phosphate groups.

	A	B
Zinc Chloride: $\text{ZnCl}_2$	10%	8%
Lithium Chloride: $\text{LiCl}$	15%	12.5%
Potassium Acetate: $\text{KC}_2\text{H}_3\text{O}_2$	20%	23.5%
Calcium Chloride: $\text{CaCl}_2$	32.3%	32.5%
Zinc Nitrate: $\text{Zn}(\text{NO}_3)_2$	42%	41%
Sodium Bisulfate: $\text{NaHSO}_4$	52%	55%
Sodium Nitrate: $\text{NaNO}_2$	66%	60%
Sodium Chlorate: $\text{NaClO}_3$	75%	71%
Potassium Bisulfate: $\text{KHSO}_4$	86%	82%

Figure 6. Humidities maintained by saturated solutions of inorganic compounds. Column A, handbook values (15), given for 20°C. Column B, measured values at room temperature, 21° ± 2°C.

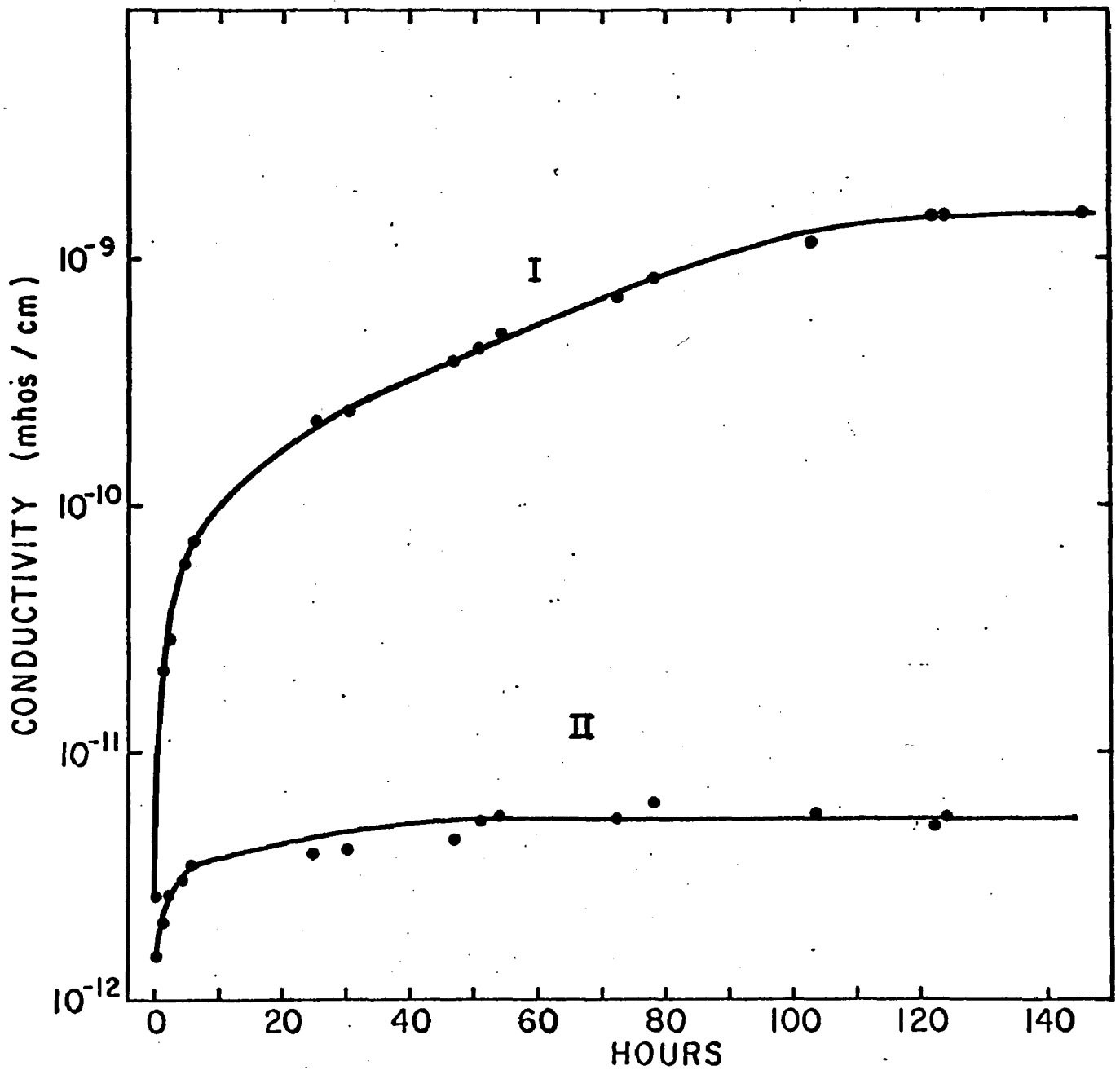


Figure 7. Conductivity of bone as a function of time. Both samples were initially vacuum dried. I shows equilibrium being attained with 98% RH, II with 50% RH.

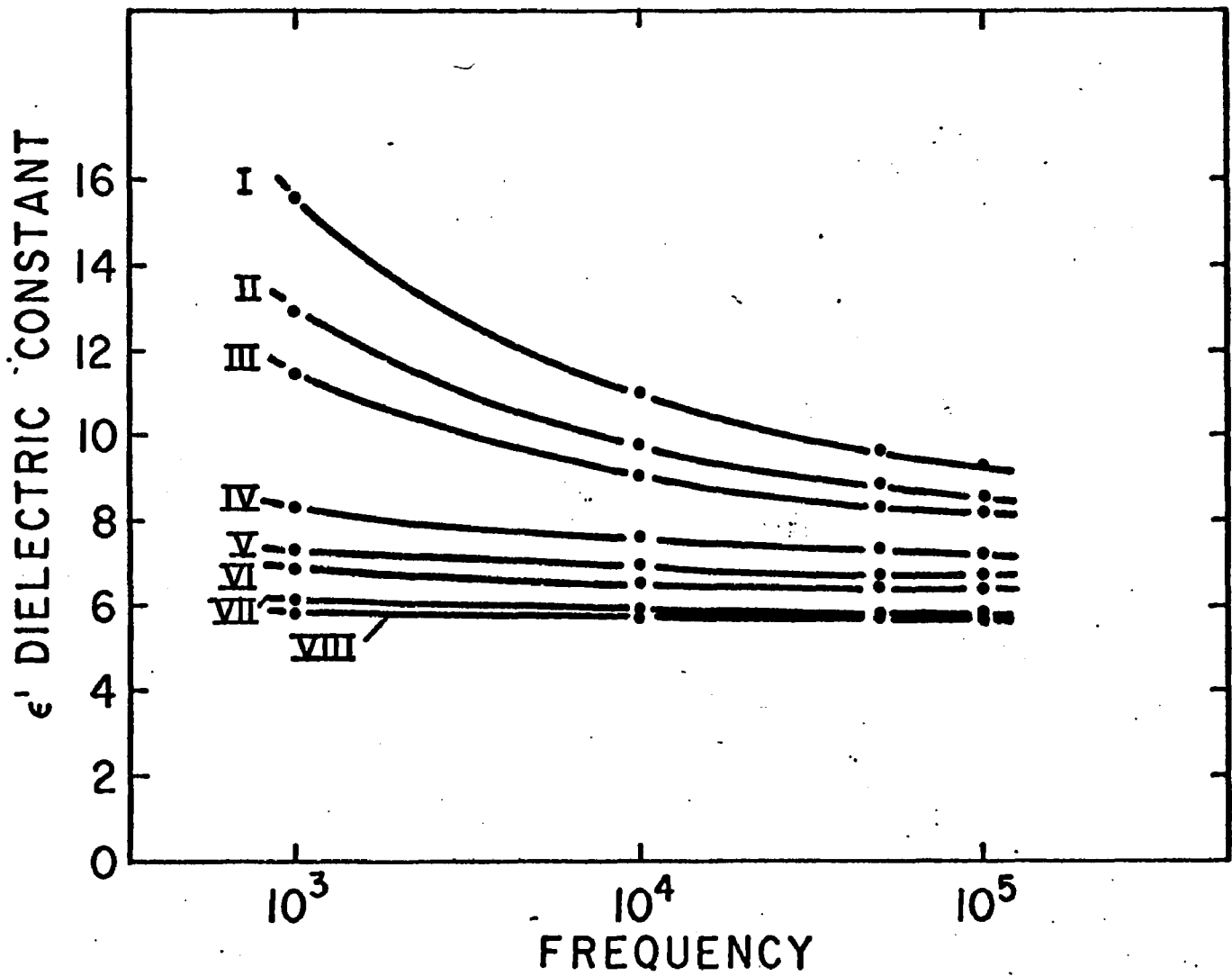


Figure 8. Dielectric constant of bone as a function of frequency (in c.p.s.) with a hydration (in mg H<sub>2</sub>O/g-bone) of: I-61.6; II-56.4; III-53.8; IV-39.8; V-29.9; VI-21.4; VII-7.0; VIII-0.

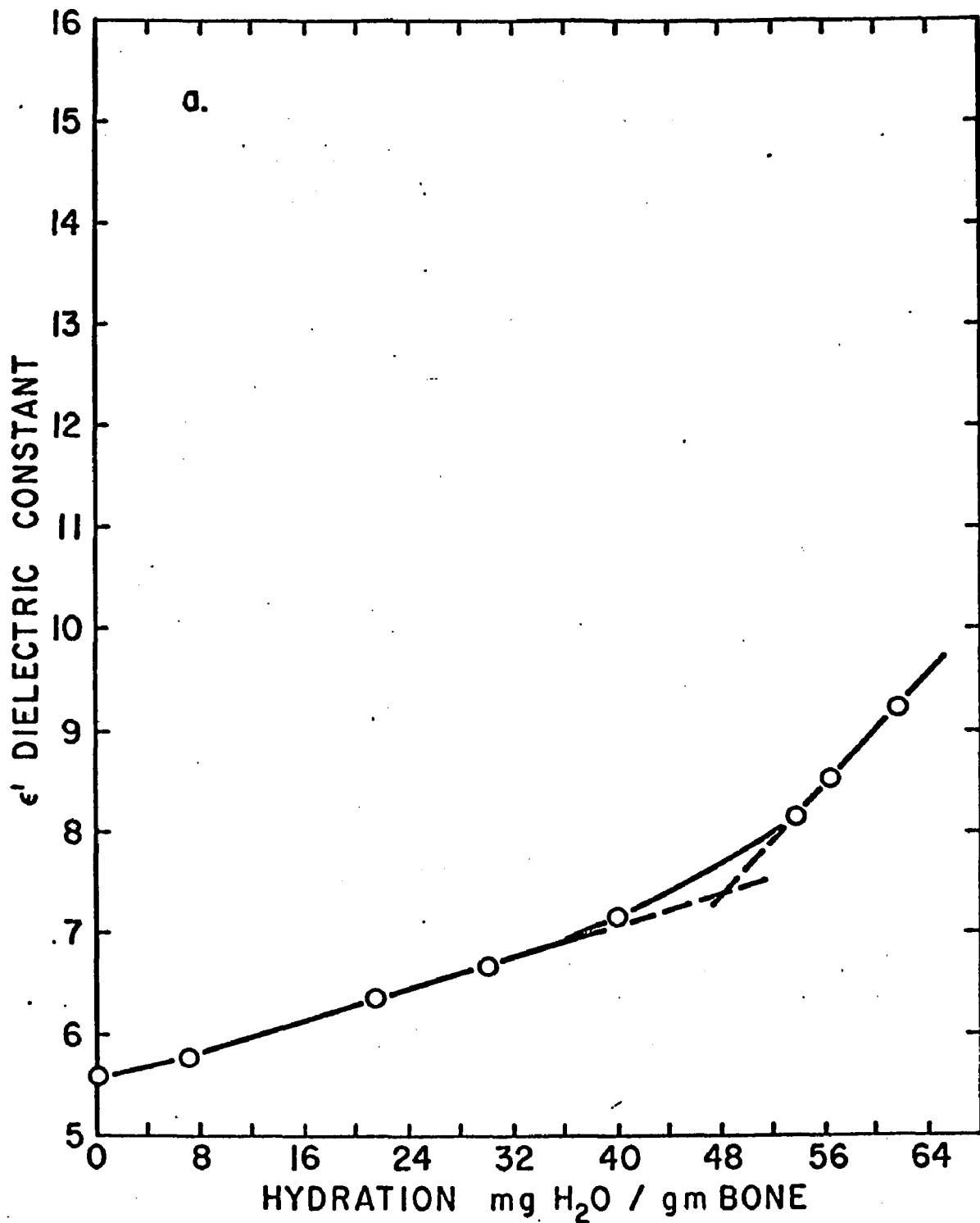


Figure 9. Dielectric constant of bone as a function of hydration:

(a) 100 kc, (b) 10 kc, (c) 1 kc.

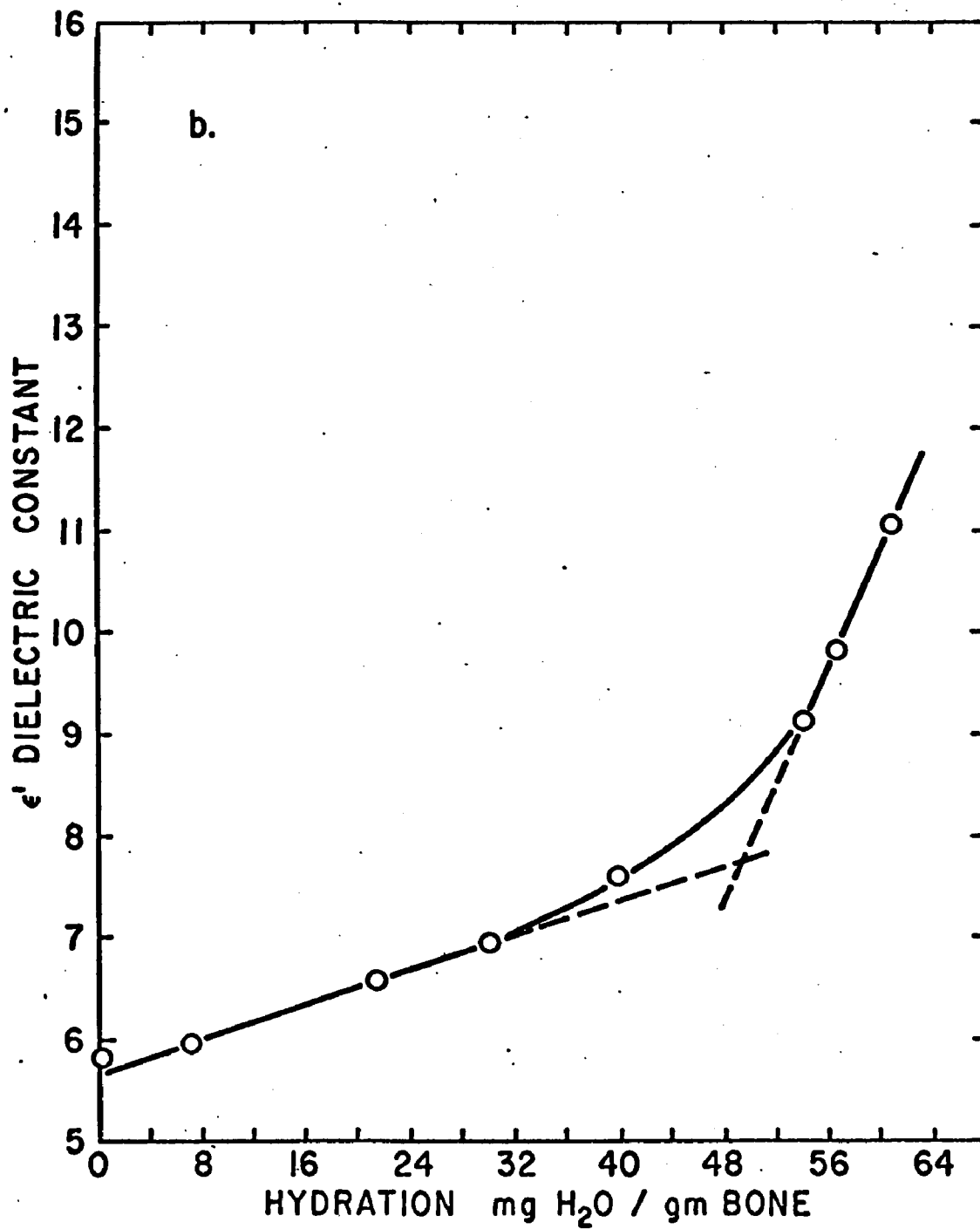


Figure 9b

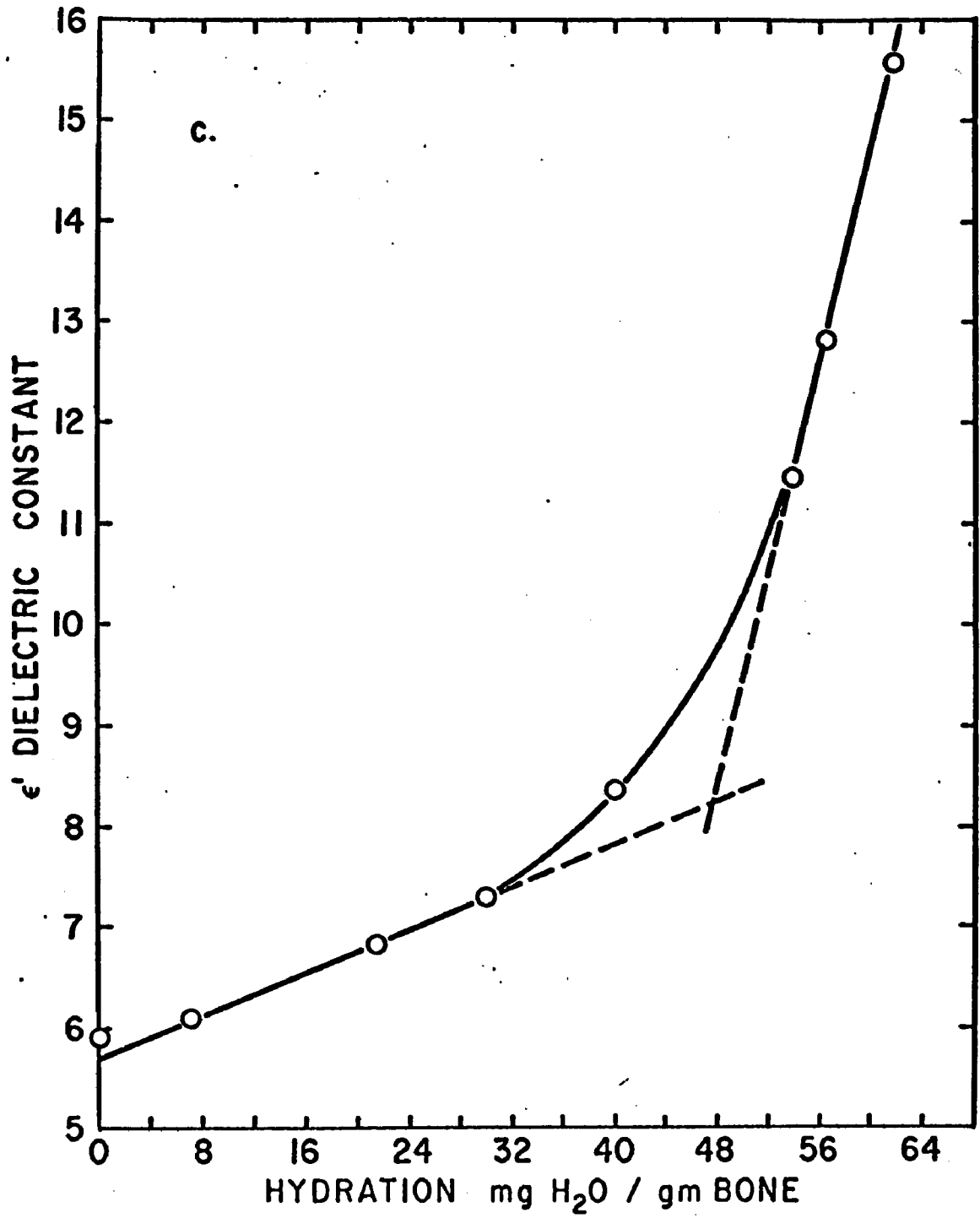


Figure 9c

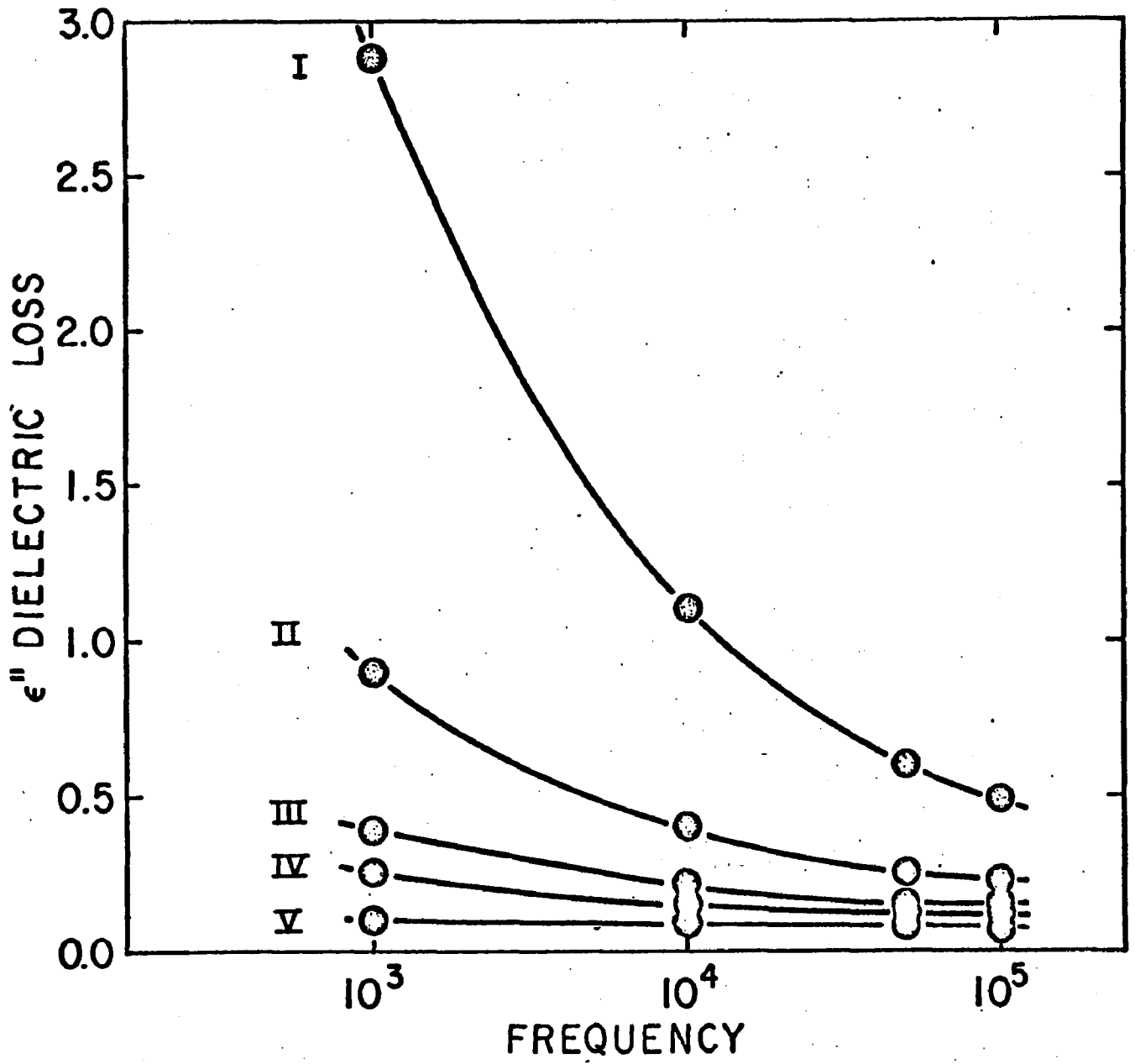


Figure 10. Dielectric loss of bone as a function of frequency (in c.p.s.) with a hydration (in mg H<sub>2</sub>O/g-bone) of: I-53.8; II-39.8; III-29.9; IV-21.4; V-0.

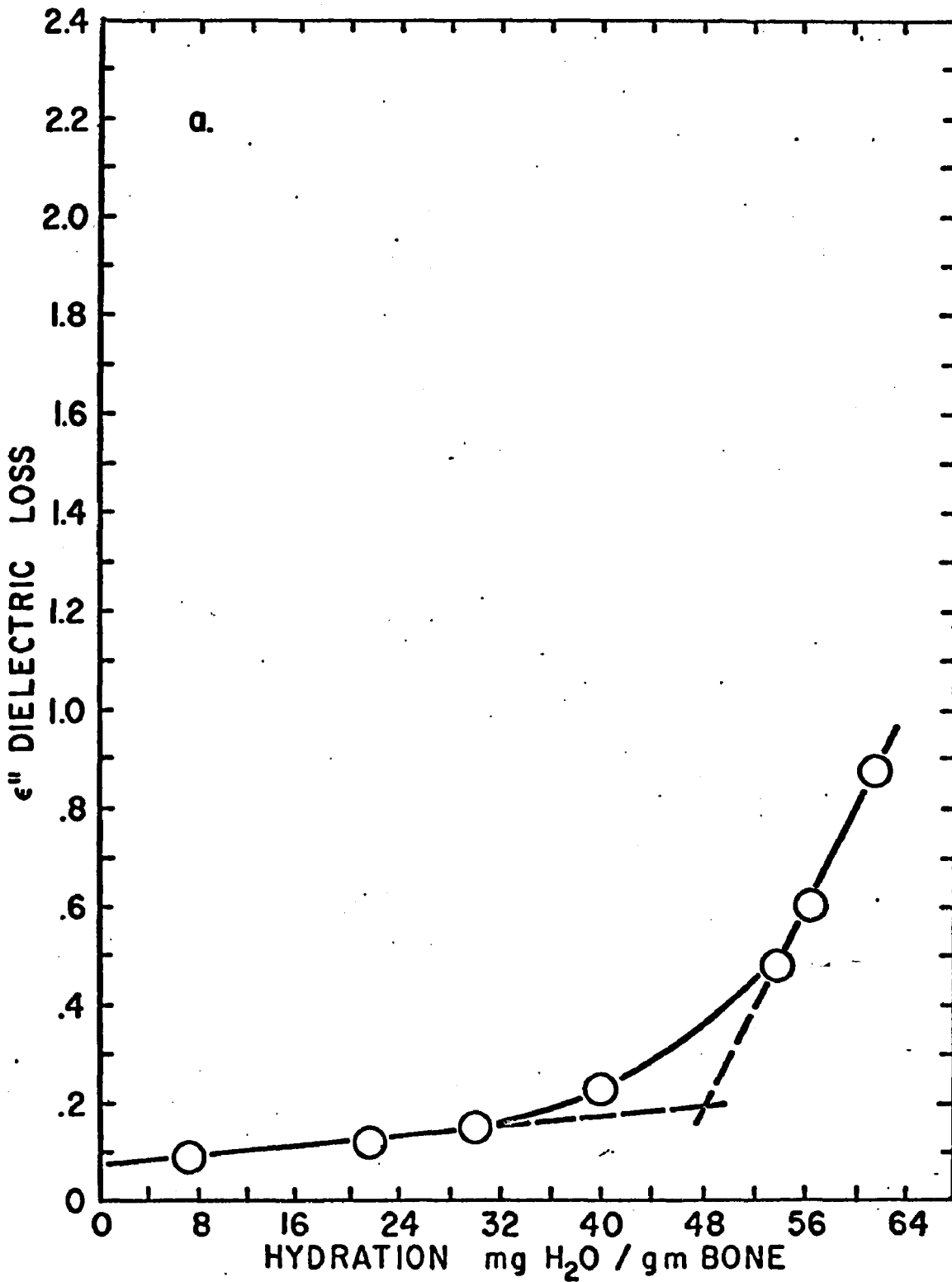


Figure 11. Dielectric loss of bone as a function of hydration:  
 (a) 100 kc, (b) 50 kc, (c) 10 kc.

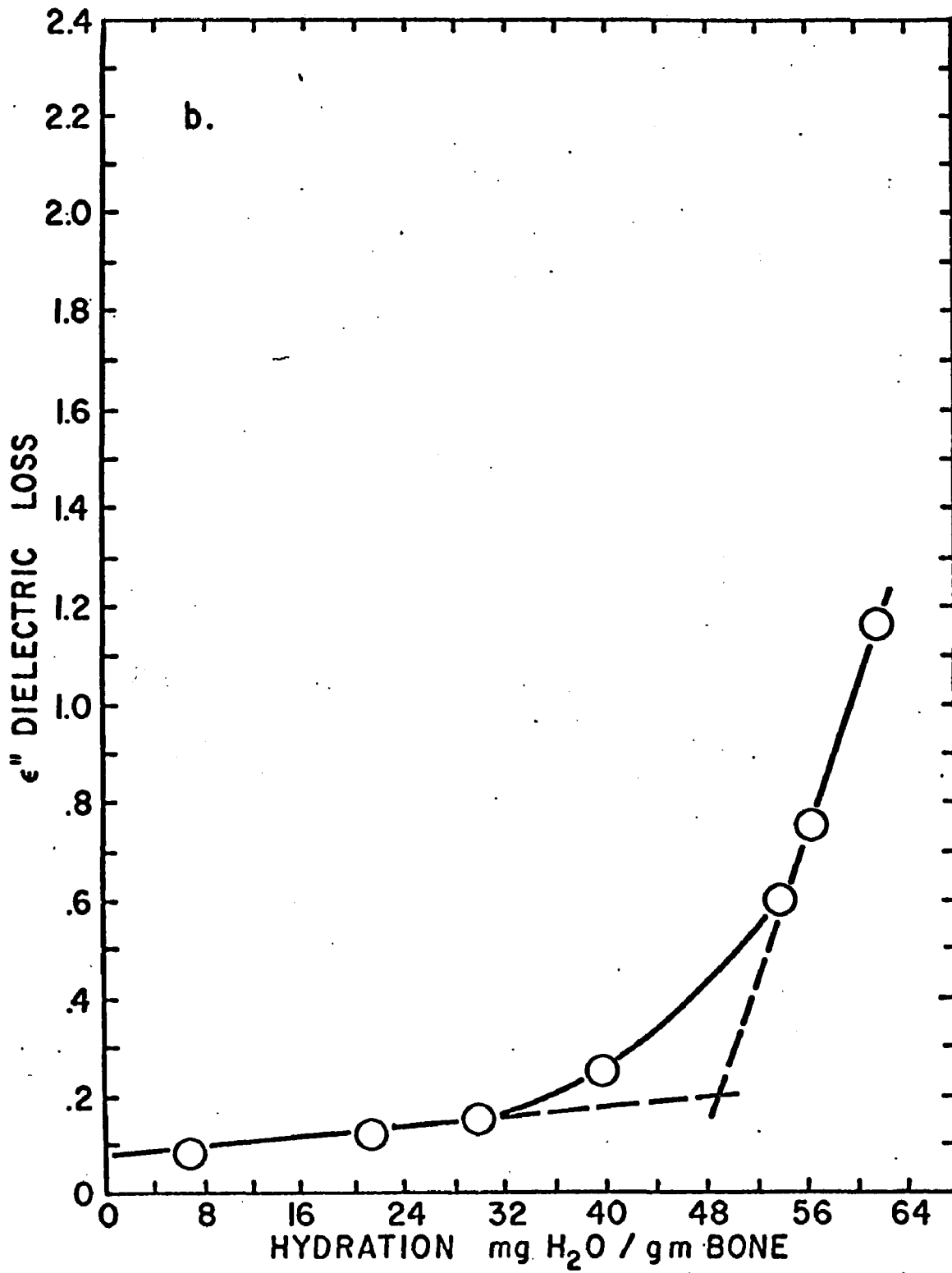


Figure 11b

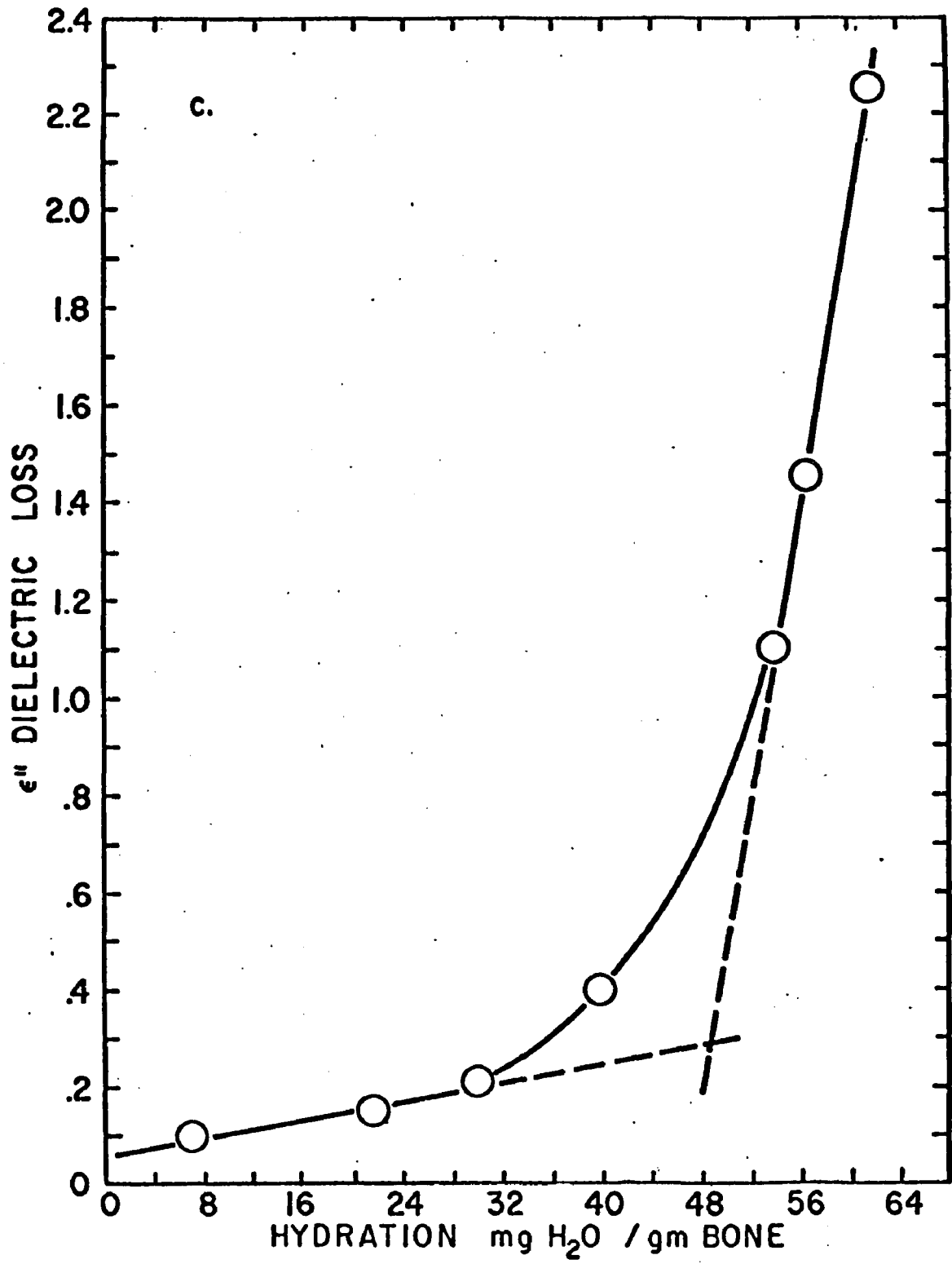


Figure 11c

Sample Number	Density (g/cc)	$\epsilon'$ Dry Bone; (Measured)	$\epsilon'$ Dry Bone; (Extrapolated)	$h_c$ (mg H <sub>2</sub> O/g-bone)
1	1.76 ± .01	5.7	5.6	48 ± 1
2	1.86 ± .01	5.8	5.7	42 ± 4
3	1.88 ± .02	6.0	5.9	46 ± 2
4	1.89 ± .02	6.3	5.6	45 ± 2
5	1.90 ± .02	6.5	6.3	37 ± 5

Figure 12. Measured and extrapolated values of dielectric constant of dry bone, and the critical hydration. Values are averaged over frequencies 100 kc, 10 kc, 1 kc.

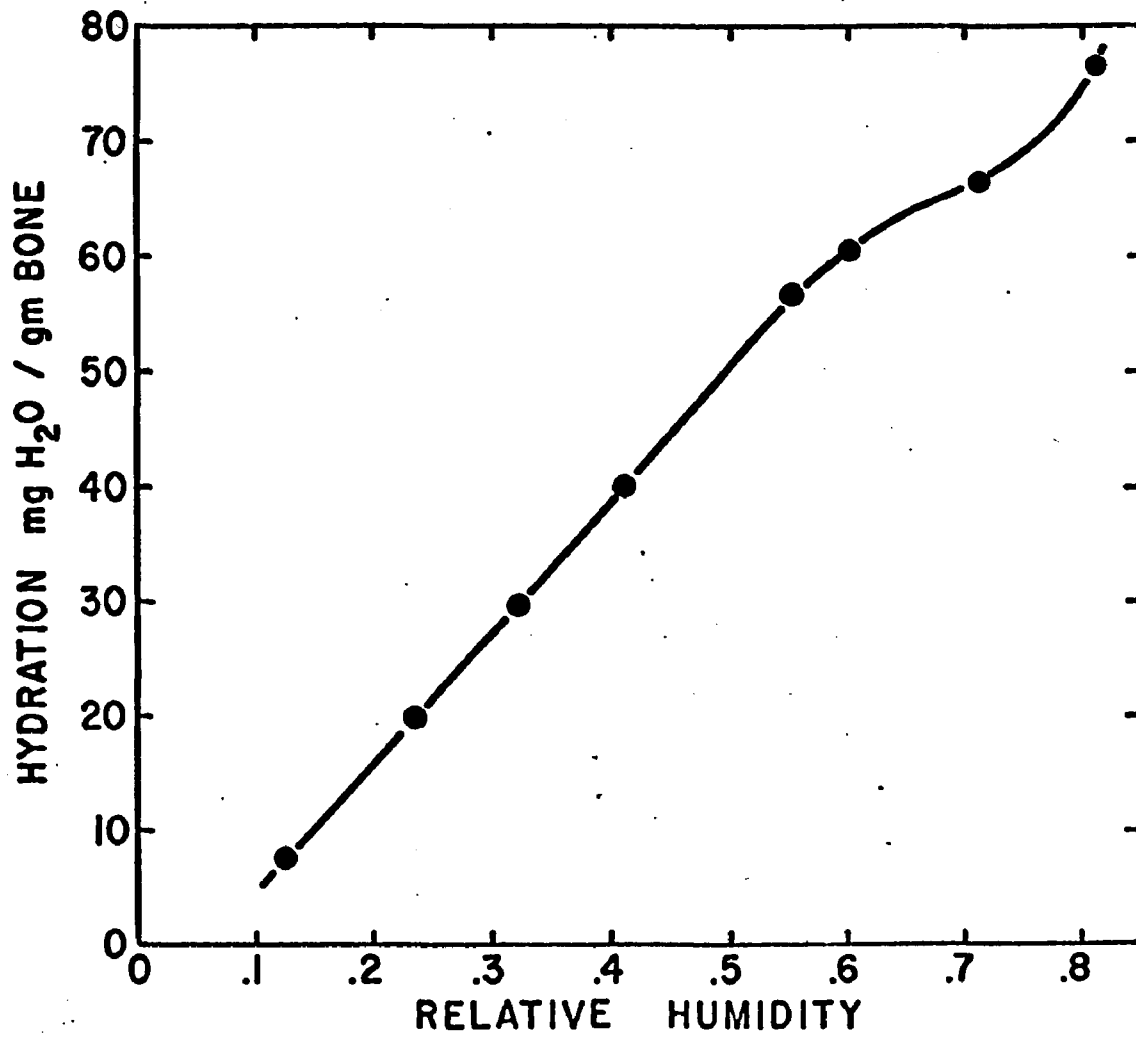


Figure 13. Average absorption isotherm of bone. Temperature,  $21^{\circ}\text{C} \pm 1^{\circ}\text{C}$ .

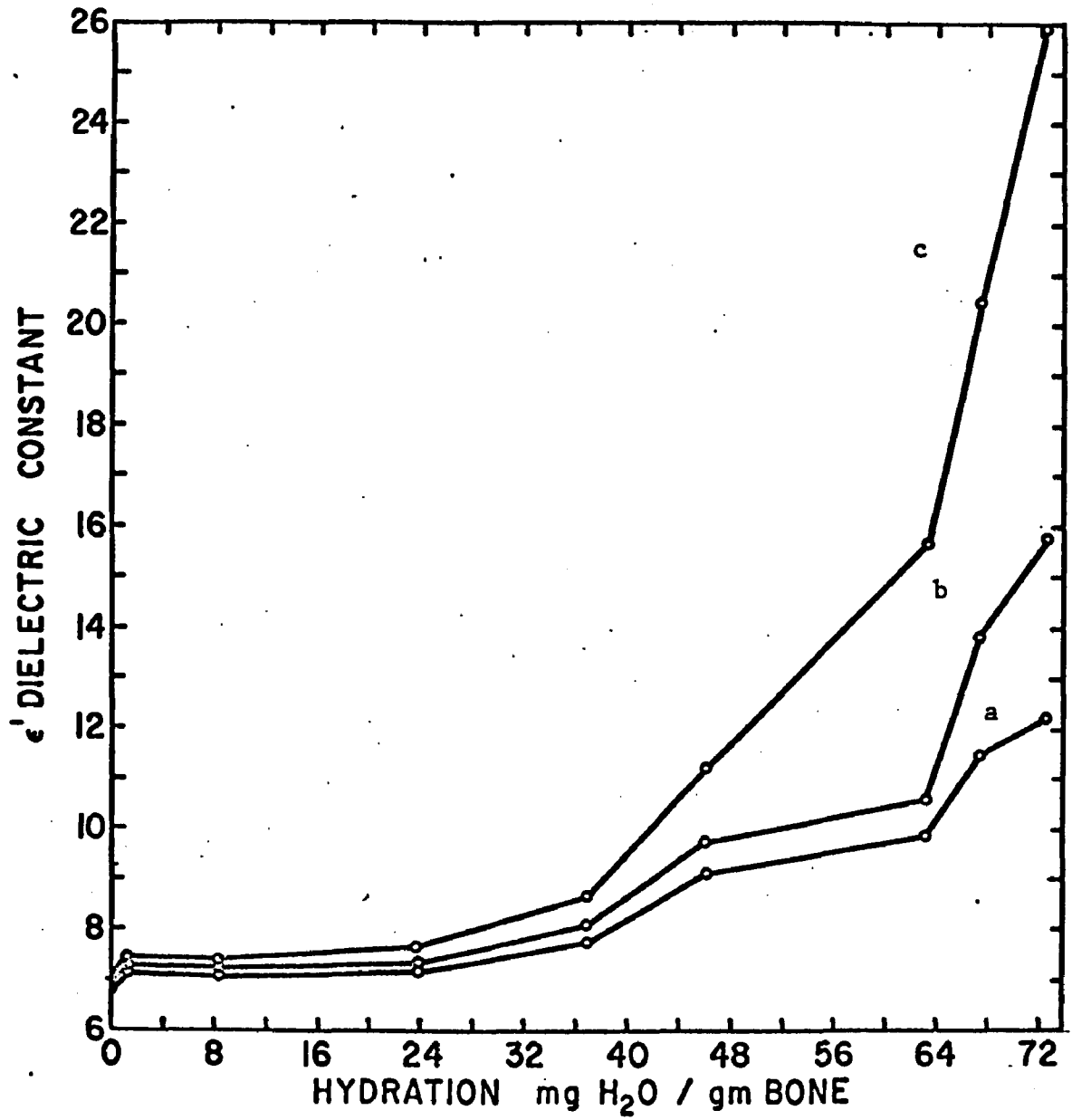


Figure 14. Dielectric constant of a sample of pathological bone as a function of hydration: (a) 100 kc, (b) 10 kc, (c) 1 kc.

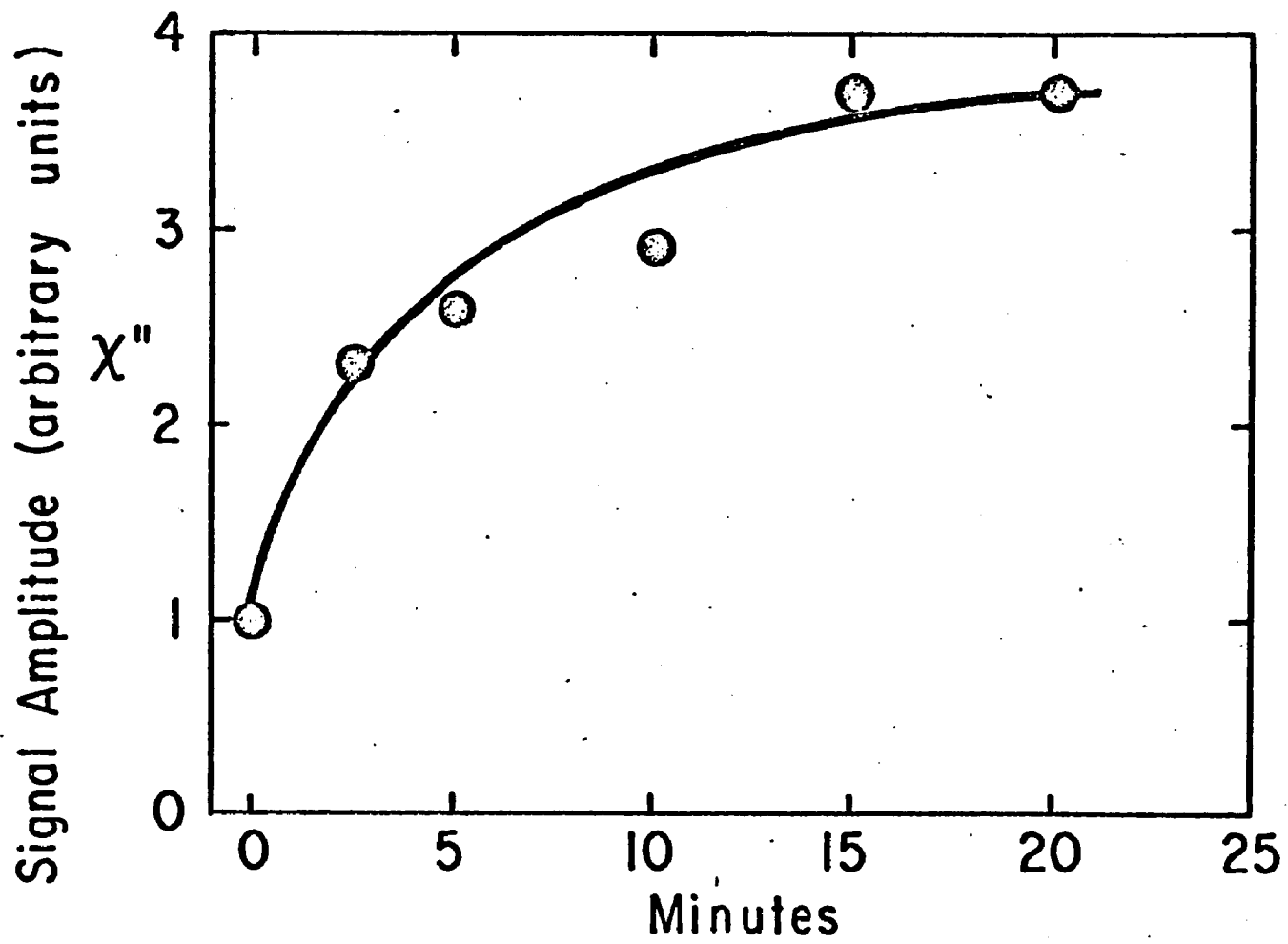


Figure 15. Accumulation of free radicals in bone powder as a function of time of dispersion.

<u>ELEMENT</u>	<u>CONCENTRATION</u>	<u>NO. OF SPINS*</u>
Titanium	N.D. (50)	$<6.3 \times 10^{17}$
Vanadium	2.5	$3.0 \times 10^{16}$
Chromium	0.5	$5.8 \times 10^{15}$
Manganese	2.5	$2.7 \times 10^{16}$
Iron	7.0	$7.5 \times 10^{16}$
Cobalt	N.D. (1.5)	$<1.5 \times 10^{16}$
Nickel	2.5	$2.6 \times 10^{16}$
Copper	9.5	$9.0 \times 10^{16}$

Figure 16. Iron group elements found in human tendon collagen by emission spectroscopy. Results are given in parts per million of air dried tendon to an estimated accuracy of 25%. For those elements not detected, the limits of detection are given.

\* Under the assumption that the element is 100% present as the paramagnetic ion of the respective species.

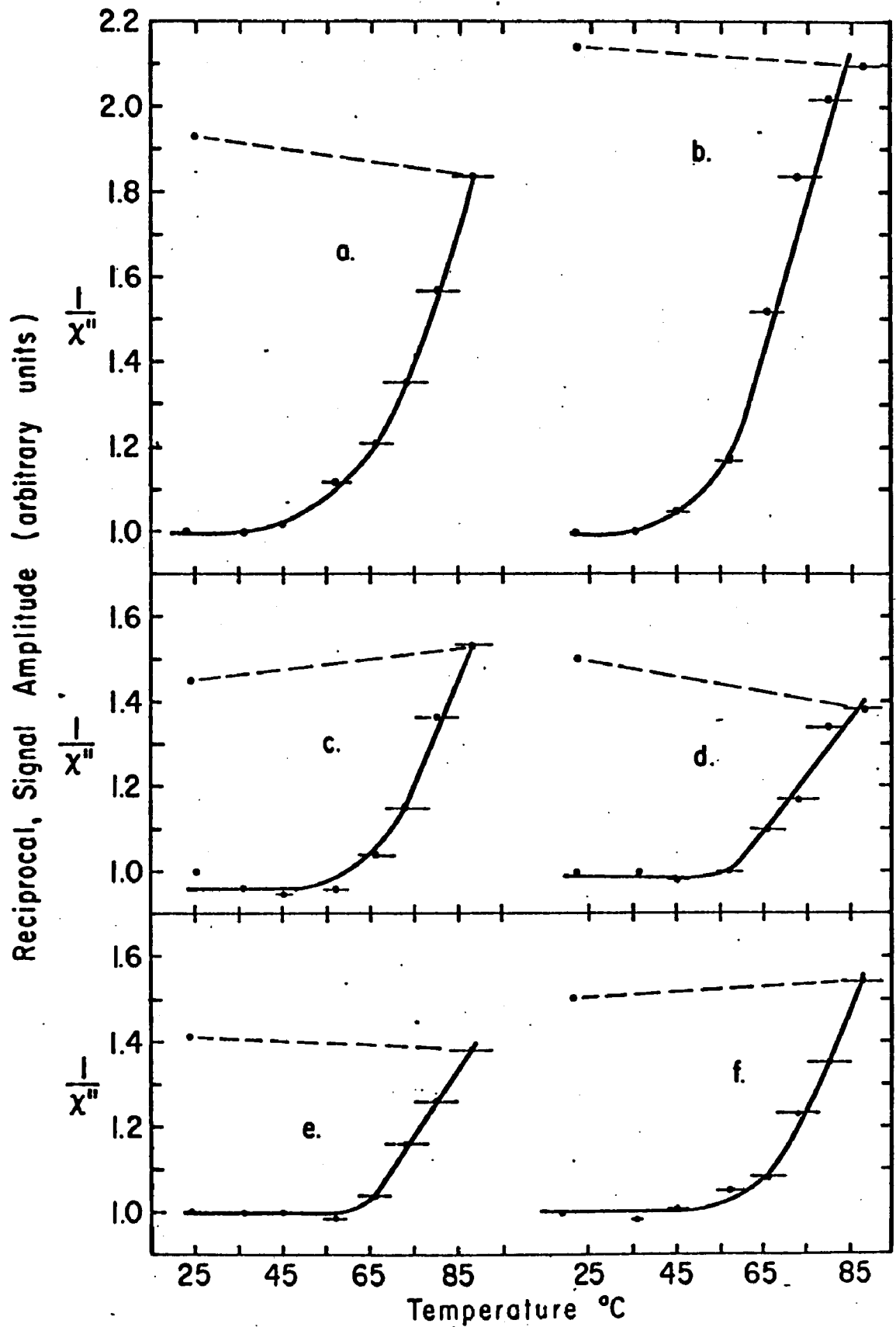


Figure 17. Temperature dependence of reciprocal of signal amplitude from tendon collagen. (a) and (b) in air, (c) and (d) in nitrogen, (e) and (f) in oxygen. The curves on the left were found initially, the curves on the right after storage for two weeks in the indicated atmosphere.

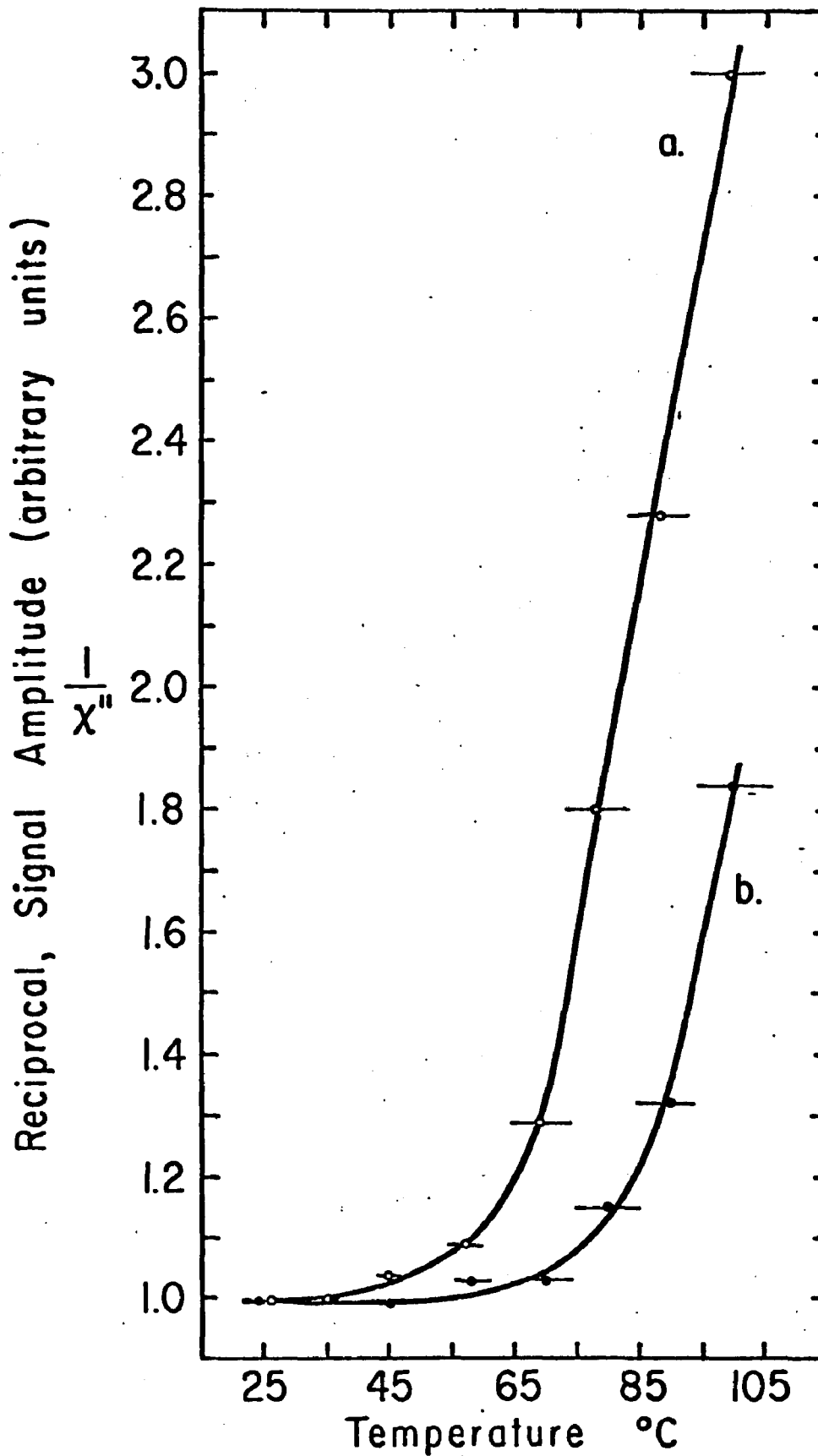


Figure 18. Temperature dependence of reciprocal of signal amplitude from gelatin. (a) equilibrated with room humidity, (b) vacuum dried at  $10^{-6}$  Torr and heated in a nitrogen atmosphere.

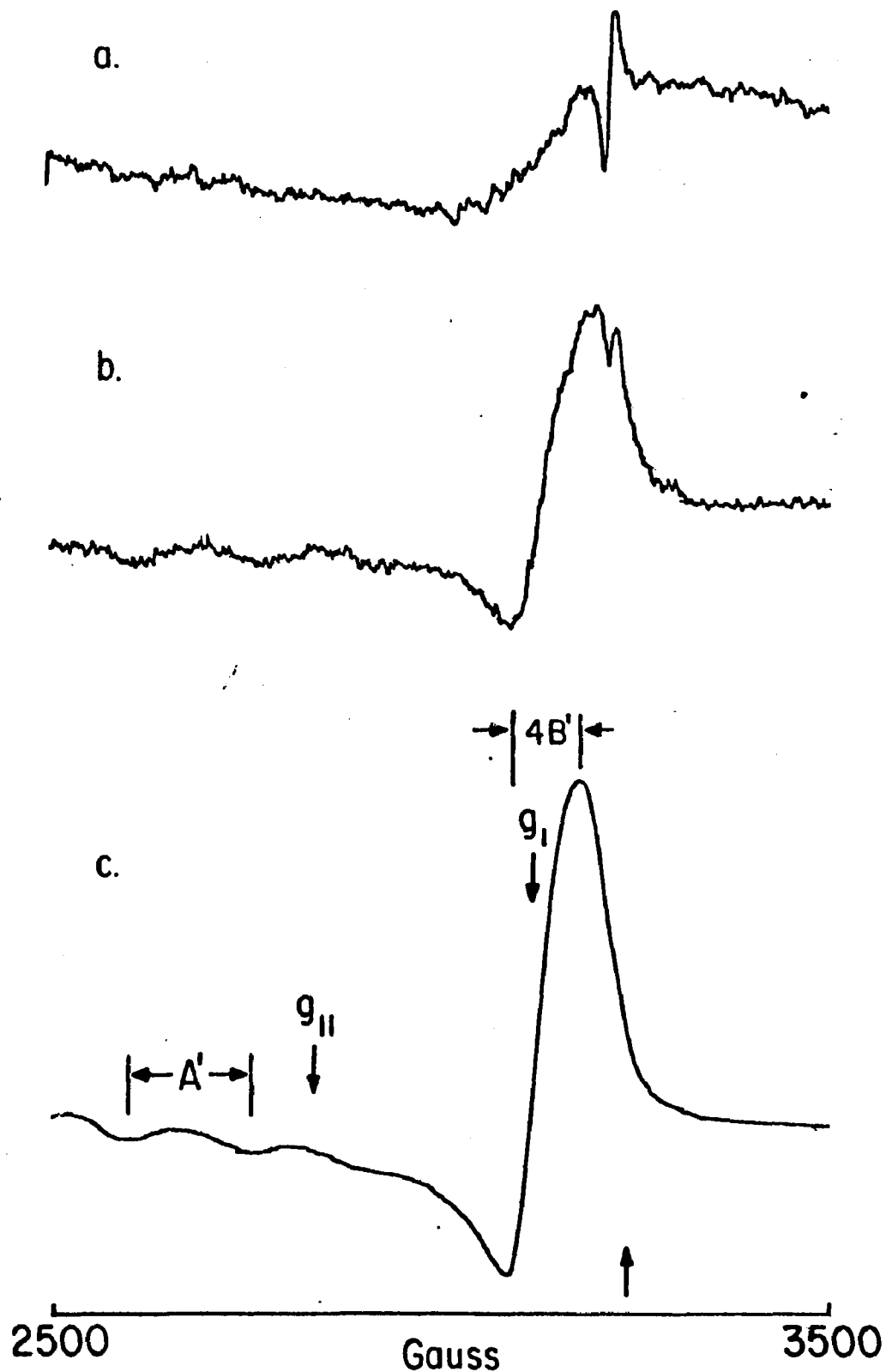


Figure 19. EPR spectrum from tendon collagen, (a) immersed in pure water, (b) in mammalian ringer's solution, (c) in a 38  $\mu\text{M}$  solution of  $\text{CuSO}_4$ . Here and in succeeding illustrations, the arrow denotes the position of  $g = 2.00$ .

<u>ELEMENT</u>	<u>CONCENTRATION</u>
Titanium	N.D. (50)
Vanadium	3.0
Chromium	N.D. (0.5)
Manganese	N.D. ((0.5)
Iron	2.0
Cobalt	N.D. (0.5)
Nickel	N.D. (0.5)
Copper	<0.5

Figure 20. Iron group elements found in bone mineral by emission spectroscopy. Results are given in parts per million of air dried bone mineral to an estimated accuracy of 25%. For those elements not detected the limits of detection are given.



Cu(II) MOLARITY	COPPER UPTAKE	
	( $\mu\text{g/g}$ )	(no. of spins/g)
0.000 mM	<0.5*	$<5.0 \times 10^{15}$
0.034 mM	$56 \pm 5$	$5.5 \times 10^{17}$
0.096 mM	$262 \pm 7$	$2.6 \times 10^{18}$
0.160 mM	$337 \pm 7$	$3.2 \times 10^{18}$
0.350 mM	$325 \pm 25$	$3.2 \times 10^{18}$

\* Naturally present copper.

Figure 22. Copper uptake of intact samples of bone mineral as a function of the molarity of the solution. Results are given as micrograms of copper per gram of air dried bone mineral, and as number of spins per gram of air dried bone mineral.

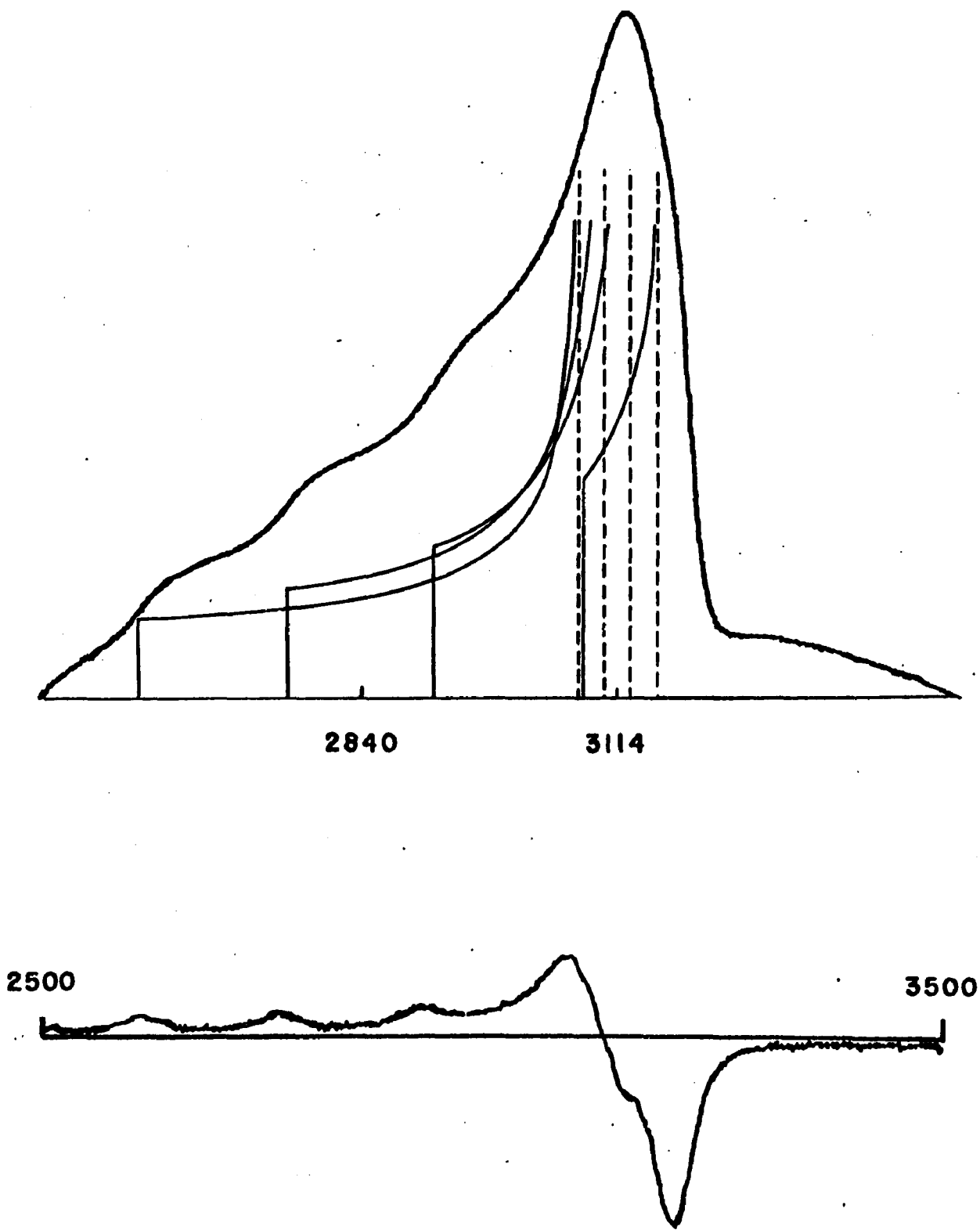


Figure 23. Derivative and integrated EPR spectrum of Cu(II) adsorbed on apatite. The theoretical distribution of line centers of the four Cu(II) hyperfine lines is shown below the integrated absorption curve.

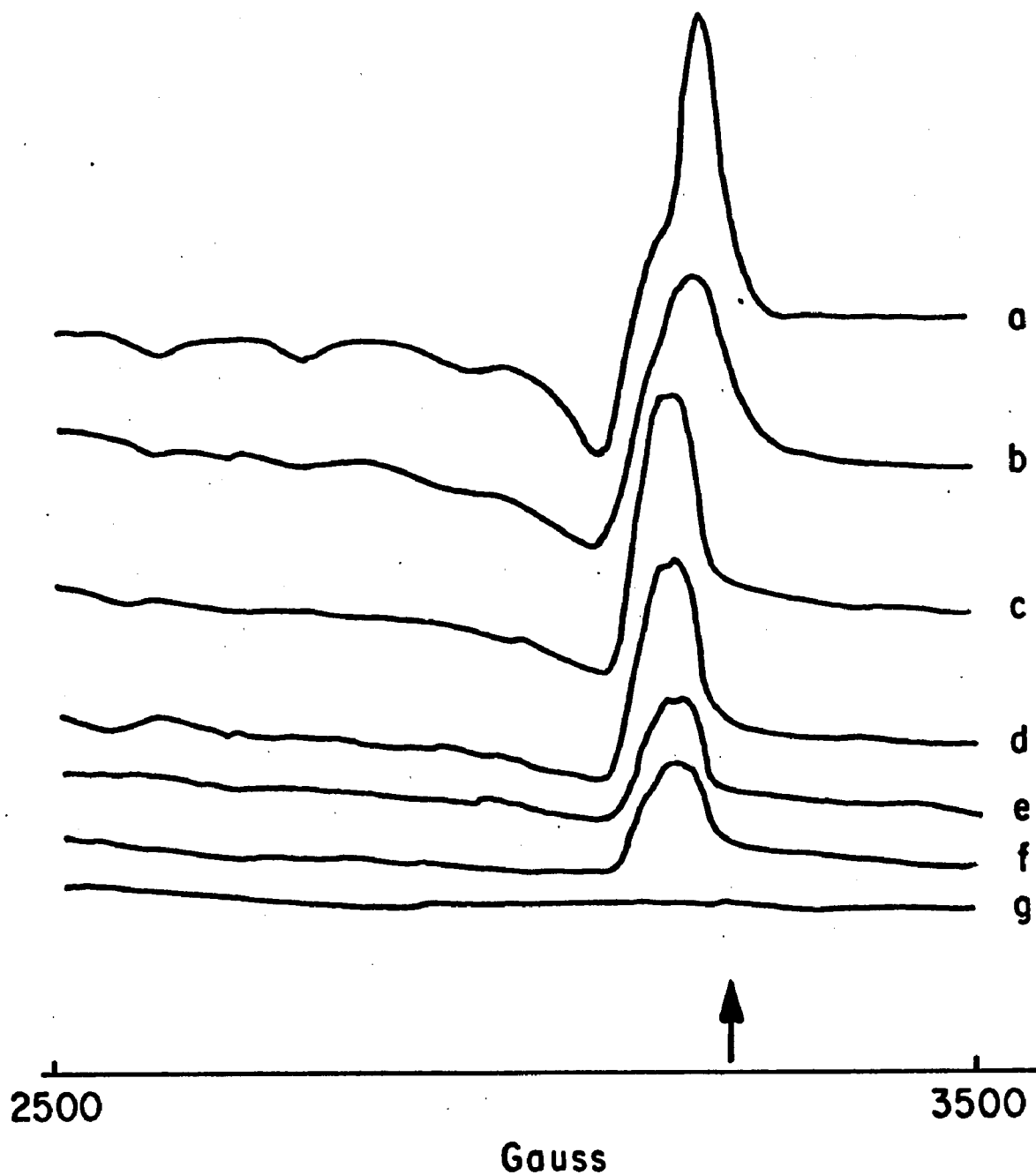


Figure 24. Change in EPR spectrum of Cu(II) adsorbed on apatite produced by heating. (a) room temperature, (b) to 110°C, (c) 200°C, (d) 300°C, (e) 400°C, (f) 500°C, (g) 600°C. Each curve was recorded after heating at the indicated temperature for twenty-four hours. The char signal, which is resolved in (c) through (f), has been deleted.

	$g_1$	$g_{11}$	A*	B*	ref.
Laccase	2.048	2.197	90	--	(23)
Ceruloplasmin	2.056	2.209	80	--	(23)
Glass	2.06	2.32	157	23	(35)
Collagen, Apatite	2.07	2.27	170	<20	
DNA, RNA	2.08	2.35	153	<30	(18)
Dowex-50	2.099	2.40	128	--	(22)

\* ( $\times 10^{-4} \text{ cm}^{-1}$ )

Figure 25. Representative values of the constants in the spin Hamiltonian which describes the powder spectrum of the absorbed cupric ion.